Journal of Materials Chemistry A

Accepted Manuscript

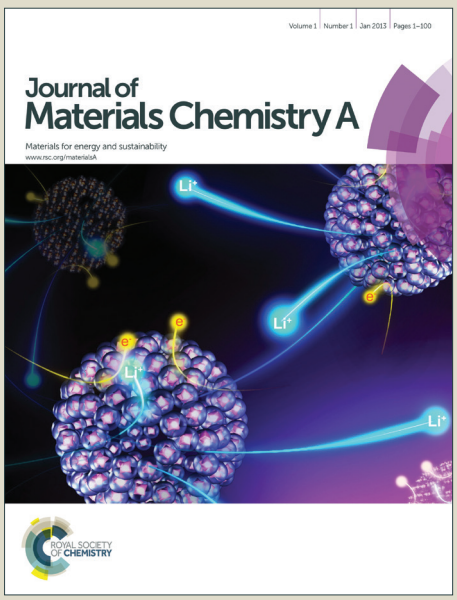

ROYAL SOCIETY OF CHEMISTRY

www.rsc.org/materialsA

Porphyrins in carbon dioxide capture and conversion: A review

Santosh Kumar*, Mohmmad. Y. Wani, Cláudia T. Arranja, Joana de A. e Silva, B. Avula, Abilio J. F. N. Sobral*

Departamento de Quimica, FCTUC, Universidade de Coimbra, Coimbra 3004-535, Portugal

*Corresponding authors: Tel.: +351 239854476 e-mail: asobral@ci.uc.pt (Abilio Sobral); santoshics@gmail.com;santosh.kumar@uc.pt (Santosh Kumar)

ABSTRACT

Uniqueness of properties and robustness of structure makes porphyrins nature's favorite catalysts. They have grabbed human attention since decades due to its intense colours and in modern times the interest in these molecules has sharply increased, owing to their use for handling some tough problems, including medical and environmental issues. Nowadays much attention is being focused on the development of materials for the capture and conversion of CO_2 into value added products and porphyrins are not lagging behind in extending their favor. The idea that porphyrins are poor absorption materials since are generally plnar compounds has been belied by the development of new efficient porphyrin-based materials, and the development of reliable synthetic routes for porphyrin based nanoreactors such as covalent-organic frameworks (COF) and metal-organic frameworks (MOF) as porous materials has facilitated to overcome the underlying CO_2 reactivity challenges. Porphyrin-based materials behaving as nanoreactors are very promising for CO_2 capture and conversion due to the presence of basic pyrrole containing macrocyclic cavity and large aromatic rings which facilitates strong interactions with CO_2. This review is intended to provide an overview of up-to-date progress made in the area of the CO_2 capture and conversion involving porphyrin-based molecular materials and nanoreactors, bearing important structural features in terms of surface area, porosity, CO_2 uptake and the possibility of its catalytic conversion to chemically valuable products.

Contents

1 Introduction

Despite the crucial importance of CO_2 (carbon dioxide) in keeping earth's temperature and atmosphere balance, which in turn is vital for life on our planet, antropogenic carbon dioxide is the primary greenhouse gas that is responsible for global warming, rising sea levels and increasing acidity of the oceans. World energy-related carbon dioxide emissions will rise from 31.2 billion metric tons in 2010 to 36.4 billion metric tons in 2020 and 45.5 billion metric tons in 2040; an increase of 46 percent over the projection period.[1] One long considered strategy to reduce atmospheric CO_2 content is CCS (carbon capture and storage), which is assumed to considerably

reduce the CO_2 concentration *via* storage. Capture, sequestration and conversion of the atmospheric CO_2 is still an open challenge for the society. In order to avoid catastrophic consequences of global warming, the development of new strategies and technologies for CCS and CCC (carbon capture and conversion) is a key research goal nowadays. The capture and storage of CO_2 has been extensively studied using a wide range of porous materials[2-5] . Among them there was porphyrins, however, the innicial lower CO_2 adsorption capacity compared to other porous materials like microporus carbons and zeolites has hampered the use of porphyrins in CO_2 capture. The use of porphyrin-based materials like MOF's, COF's and other porphyrin linked polymer materials, have, however comeup in the last years with enhanced CO_2 adsorption profiles, which deserves our attention. The unique structural properties including robustness, high thermal and chemical stabilities, unpresendeted internal surface areas (up to 5000 m^2g^{-1}), high void volumes (55-90 %), low densities (from 0.21-1.00 gcm^{-1}) and the ability to modelate the pore dimensions and surface chemistry within the organic frameworks are some features which are not available in most of other porous materials.[6]

Carbon dioxide on the other extreme is considered as an attractive, highly functional, abundant, inexpensive, nontoxic, and nonflammable C1 building block in organic synthesis. It can be used as an everlasting chemical feedstock for the production of high value products. In this pursuit CO_2 has been successfully used in the large scale production of useful organic chemicals and highly reactive substrates, including epoxides, urea, salicyclic acid and several carbonate-based materials using catalysts of varied nature.[7] This is an active area of research and has been reviewed by other authors,[8,9] but the use and scope of porphyrins as nanoreactor systems in the selective conversion of CO_2 have not received much attention, possibly due to the availability of other metal catalyzed systems for the conversion of CO_2 to useful products. Following our work on the CO_2 capture[10] with porphyrins[11] and porous porphyrin-based materials,[12-15], in this review we highlight the importance to study and investigate the porphyrin systems for CO_2 capture and conversion, which can act as

nanoreactors for the conversion of CO_2 to industrially useful products efficiently and with high selectivity.

2. Porphyrins as nanoreactors

Porphyrin nucleus consist of four pyrrole rings joined by four methine bridges to give a near planar macrocycle, based in a 18 π-electronic conjugated network. Porphyrin and its derivatives decorated with self-assembled motifs have been widely used as molecular scaffolds for the construction of well defined organic nanostructures. They can be easily incorporated into an organic framework by forming inter-links with rigid units and forming porous organic polymers due to the unique macrocyclic structure of the porphyrin. The porphyrins in the framework can bind various metal ions to form heterogeneous metallo-porphyrin catalysts. These characteristics of the porphyrins have been utilized in the preparation of MOFs of high porous structure, where CO_2 molecules can interact with multiple pore surfaces simultaneously, as in a nanoreactor. Hence showing an enhanced CO_2 adsorption, as well as efficient and selective conversion to useful products (**Fig. 1**).

Nanoreactors, as promising upcoming technologies have been used to solve numerous challenges met by researchers worldwide.[16-19] A nanoreactor is a nanosized container, which provides enormous advantages compared to the macroporous materials.[20] The reaction space inside a nanoreactor in terms of reactive species over the nanoreactor walls strongly influences the movement and interaction of captured molecules. The nanoreactor can not be regarded simply as a holding vessel, but is a critical part of the chemical process. In general, as the dimensions become smaller, the reacting molecules in the inner space increasingly interact with the surface and to each other resulting in a big difference between the reaction kinetics in confined space and in bulk. Besides, the arrangement of molecules and ions inside the nanoreactors are nonrandom and this has profound consequences on the chemical processes that may take place inside. Porphyrins, with its confined dimensions of the core containing chemically reactive amine functional group act as nanoreactors,

which could be selectively used for the chemical adsorption and conversion of CO_2, thus providing an added benefit compared to the other materials used for CO_2 capture and conversion.[6]

The quest for the fundamental understanding of nanoreactors and their wide range of applications in chemical transformations and in chemical synthesis has led to the design and construction of a wide range of specific models. These include self-assembled nanoreactors,[21,22] microemulsion nanoreactors,[23,24] hybrid organic-inorganic sol-gel nanoreactors,[25] protein polymer nanoreactors,[26] immobilized protein-polymer nanoreactors,[27] hydrogel nanoreactors,[28,29] inorganic nanotubes as nanoreactors,[30] mesoporous silica nanoreactors,[31] shell cross-linked micelle-based nanoreactors,[32] virus-based single enzyme nanoreactor[33] and cyclodextrin nanoreactors.[34] The efficiency of a chemical process in the nanoreactor is enhanced by the availability of reliable and highly efficient microstructured materials within sub-millimeter ranges. The extremely large surface-to-volume ratio in nanoreactors enhance heat and mass transfer dramatically, and hence provide many potential opportunities in chemical conversion of desired materials. The development of nanoreactors has been followed by the development of new theoretical models of interpretation, like the Confined Reaction Fields Theory (CRF) developed by Polarz and Kuschel in 2008.[35] CRF correlates kinetic and thermodynamic parameter inside nanoreactors and other confined spaces and successfully predicts and interprets data from several reactions in different nano environments, ranging from 2 to 28 nm.[35-38] However, this subject is beyond the scope of this review.

3. Types of porphyrin-based materials for CO_2 capture

The main body of work on porphyrin-based materials for the CO_2 capture is based in porous materials that present the adequate geometry and inner chemical surfaces able to adsorb CO_2 reversibly.[6,39] The absorption profile of different kinds of materials has been discussed elsewhere and readers are directed to read the review.[39] Here we discuss porphyrin-based materials, like MOFs, COFs and porphyrin linked porous polymer materials developed in the last decades to enhance the

CO_2 capture profile of the porphyrins, which were previously considered to be less efficient, compared to the other porous materials. Yagi's group[40] first reported the use of MOF's in CO_2 capture at room temperature, followed by development of new types of MOFs, and since then the field is enormously growing.[39]

3.1. Metal-organic frameworks

In the past two decades, a new class of crystalline porous material namely metal-organic frameworks (MOFs) has emerged as a leading field of research in one of the most prolific areas in chemistry of materials science.[41,42] MOFs as nanoporous crystalline materials are formed by reticular synthesis, which creates strong bonds between inorganic and organic units. Careful selection of MOF constituents can yield crystals with ultra porosity and high thermal and chemical stability. This unique class of porous hybrid solids has a wide range of compositions, structures, tunable pore size, and pore volume, which could serve as an ideal platform for the development of next generation CO_2 capture materials owing to their relatively higher CO_2 adsorption capacity, due to their structural and chemical tenability[43-45] and comparable self diffusivity in comparison to most zeolites and carbon materials.[46] The CO_2 adsorption capacity of different MOFs and their comparison with other porpus materials has already been reviewed.[39,46] Here, we only discuss porphyrin-based materials and the recent advances.

MOFs have emerged as promising materials for CO_2 capture and sequestration from fuel gas. The adsorptive capacity is an important parameter for MOFs to enhance CO_2 capture, because one can know the amount of CO_2 that is adsorbed inside a unit mass of the porous material. The high internal surface areas of MOFs provide chance for large CO_2 adsorption capacities to be achieved, owing to the efficient packing and close approach of the guest molecules on the pore surface.[47] A big challenge to pre-design a MOF with a precise, multivalent binding environment at the molecular

level to enhance CO_2 capture, was taken by Johnson and his coworkers, who demonstrated the direct X-ray crystallographic observation of a porphyrinic MOF (UNLPF-2) containing a multivalent binding environment for capturing CO_2 (**Fig. 2**).[48] Assembled from an octatopic porphyrin ligand with $[Co_2(COO)_4]$ paddlewheel clusters, the distance of the binding sites is 6.1Å, needed to specifically capture the *in situ* generated CO_2. The Co metal in the porphyrin macrocycle dictates the formation of MOFs with a topology required for CO_2 trapping. UNLPF-2 can not only release but also recapture CO_2 generated *in situ*, that exhibits a good recyclability.

Recently, Nandi and Goldberg[49] have isolated a 2D bilayered MOF with ZnTCPP [ZnTCPP = 5,10,15,20-tetrakis(4-carboxylatophenyl)porphyrinato-zinc]$^{4-}$ linkers and multi-component inter-porphyrin connectors, with neutral molecules of CO_2 coordinated to the zinc centers within the bilayers in a rare μ^2-$\eta^2_{O,O}$ mode. No CO_2 was absorbed in a similarly structured MOF formulated with the free-base TCPPH2 ligands, indicating that zinc is essential for fixation of CO_2 in this type of materials. Remarkably similar fixation of CO_2 within bilayered MOFs of ZnTCPP has also been observed using other lanthanoid ions (Nd, Sm, Gd, Dy), while no fixation occurred in the polymeric product of a similar process involving free-base TCPPH2 and Dy ions.

Magnesium tetra-phenyl-porphyrin (MgTPP) could be used as a renewable amine-fixing agent to reduce amine losses in CO_2 capture, formed MgTPP-amine adducts.[50] The amines (diphenylamine and triethylamine) form adducts again with the regenerated MgTPP after CO_2 is released. The interactions between MgTPP and diethylamine are weak, and MgTPP hardly interacts with diphenylamine, or triethylamine because of steric hindrance. The ethylenediamine is an excellent agent for CO_2 capture because it has two amino sites and stronger Kassoc values for MgTPP. Kim et al have demonstrated the use of 1D double chain dipyridyl-porphyrin based porous coordination polymers for selective CO_2 adsoprtion.[51]

MOFs can directly incorporate a variety of metalloporphyrins (Al^{3+}, Zn^{2+}, Pd^{2+}, Mn^{3+} and Fe^{3+} complexes) to accomodate large channels and accessible active sites for CO_2 uptake.[52] With regard to

the prospects of creating new materials suitable for real world applications, the high degree of control over the structural and chemical features of metal-organic frameworks is particularly promising for optimization of their properties, not only for the type of CO_2 capture to be performed but also for the specific composition of the flue gas of a particular power plant.[47]

Wang et al. have prepared three-dimensional porous metal-metalloporphyrin framework that consists of nanoscopic rhombicuboctahedral cages with a high density of 16 open copper sites, based upon the custom-designed 5,15-bis(3,5-dicarboxyphenyl) porphine ligands that link copper paddlewheel symmetric secondary building units (SBUs).[53] The symmetric packing of the rhombicuboctahedral cages in MMPF-1 constricts its pore size, which facilitates selective adsorption of H_2 and O_2 over N_2, and CO_2 over CH_4. Gas adsorption studies at 195 K indicated that MMPF-1 can uptake a large amount of CO_2 (80 cm^3g^{-1}) at 760 Torr, which is much higher than the amount of CH_4 (18 cm^3g^{-1}).[53] Wang et al. have constructed (6,8,8)-connected porphyrin-based MOF, MMPF-2, which possesses a highest surface area.[54] The high surface area and high density of open cobalt centers of the porphyrin are rigidly arranged in a "face-to-face" configuration to form the channel walls (**Fig. 3**), which affords to CO_2 capturing. The CO_2 adsorption isotherm of MMPF-2 has an uptake capacity of 170 cm^3g^{-1} (or 33.4 wt% or 7.59 mmol g^{-1}) at 760 torr and 273K CO_2 adsorption isotherm at 298 K, observed a capacity of 101 cm^3g^{-1} (or 19.8 wt% or 3.0 mmol g^{-1}).[54] The high density of open metal sites in MMPF-2 was responsible for interaction between CO_2 and MOF frameworks.[46,47] The linkage of a custom designed tetrakis(3,5-dicarboxyphenyl) porphyrin ligand by triangular molecular building block that are generated *in situ* results in the formation of the high symmetry small cubicuboctahedron supermolecular building blocks that are the result of vertex-directed self-assembly. The MMPF-4 supermolecular building blocks are the key to the generation of two isostructural porphyrin-based MOMs, MMPF-4 and MMPF-5, that are permanently porous. The CO_2 adsorption isotherm of MMPF-4 has an uptake capacity of 124 cm^3g^{-1} (or 24.4 wt% or 5.54

mmol g^{-1}) at 273K and CO_2 adsorption isotherm at 298 K, observed a capacity of 67 cm^3g^{-1} (or 13.2 wt% or 3.0 mmol g^{-1}).[55]

3.2. Covalent-organic frameworks

Covalent-organic frameworks (COFs) are covalent porous crystalline materials that enable the elaborate integration of organic building blocks into an ordered structure with atomic precision.[56] COFs have low mass densities with high thermal stabilities and provide permanent efficient porosity. In this respect, the design strategies applied to other covalently bonded porous solids could be adapted to the COF synthesis. The molecular length of the building units determines the topology of the porous structure. In most cases, the linking groups formed are boroxines,[57] azine,[58] triazines,[59] imines[60] or hydrazones.[61] The main concern for characterising COFs include its structural regularity, atomic connectivity, porosity and morphology. In 2005, Yaghi *et al.* demonstrated the principle of the topological design and its advantages for the synthesis of porous organic frameworks (POFs) connected *via* covalent bonds, which were the first successful examples of COFs.[62] COFs can be categorized into either two-dimensional (2D) or three-dimensional (3D) COFs on the basis of building block dimensions.[62,63] 2D COFs provide the possibility of charge carrier transport in the stacking direction, which implies that 2D COFs have the potential for developing new type π-electronic and photo-functional materials for optoelectronics and photovoltaics. 3D COFs, which extend the framework three dimensionally through building blocks containing sp^3 carbons atoms, possess high specific surface areas, large pore volume, numerous open sites and also low densities. These features make 3D COFs ideal candidates for gas storage.[64,65] The gas adsorption capacity of a 3D COF depends primarily on the components and topologies of its frameworks. Theoretical simulations predict that COFs doped with alkali metals could improve gas storage capacity, which demonstrates the usefulness of introducing functional-sites for interactions with gases.[66]

In general, COFs are synthesized by solvothermal method and the synthesis of COF materials often takes 2 to 9 days under heating (80-120 ^{o}C) within a pressurized sealed vessel. The applied pressure may influence the reaction yields significantly. Incorporation of functional moieties into COFs might become a preferable choice to enhance their capacity of CO_2 storage and surface functionalities that interact strongly with CO_2, frequently increasing adsorbent capacity at low pressures. Recently, researchers have synthesized extended MP-COF (**3**), COF-66 (**6**) and COF-366 (**9**) by condensation reaction between tetra(*p*-boronic acid phenyl)porphyrin and 2,3,4,5-tetrahydroxy benzene, tetra (*p*-amino-phenyl) porphyrin and terephthaldehyde, tetra(*p*-boronic acid phenyl) porphyrin and 2,3,4,5-tetrahydroxy anthracene respectively (**Fig. 4-6**).[67,68]

COFs with highly functionalized pore wall structures are difficult to get *via* direct polycondensation reactions. The systematic pore surface engineering of COFs enables the tailor made covalent docking of a variety of different functional groups with controlled loading contents to the pore walls. The surface engineering of the pore walls intensely affects the surface area, pore size and pore volume. This approach enables the development of various tailor-made COFs with systematically tuned porosities and functionalities while retaining the crystallinity.[69] It also enables to attach a wide range of hydrophilic to hydrophobic and acidic to basic functional groups to the pore walls. Imine-linked covalent organic frameworks (**Fig. 7**) for CO_2 adsorption have been prepared by pore surface engineering.[69] The affinity and the uptake capacity for CO_2 adsorption are highly dependent on the structures of the functional groups (**Fig. 8**). The Imine-linked COFs (**Fig. 7a**) with different functional groups (**Fig. 7b**) exhibited decrease in their BET surface areas and pore volumes (**Table 1, entry 1-25**). The ethynyl group COFs with the values of X=0, 25, 50, 75, and 100 exhibited CO_2 capacity of 38, 29, 26, 24, and 20 mg g^{-1}, respectively, at 298 K and 1 bar; these capacities increased to 72, 54, 48, 43, and 39 mg g^{-1} at 273 K and 1 bar.[69] The capacity for CO_2 adsorption are highly dependent on the structures of the functional groups (Table 1 entry 1-25). The adsorption of CO_2 upon pore surface engineering is related to the interactions between functional groups and CO_2. The

nonpolar ethynyl and ethyl groups interact weakly with CO_2, resulting in their poor adsorption capacity and the polar ester units could interact with CO_2 *via* dipole interactions, thus improving the affinity of the COF for CO_2. The amino groups form acid-base pairs with CO_2, leading to a significant enhancement in CO_2 adsorption.[69]

3.3. Porous organic polymers

In recent years, porous organic polymers (POPs) have attracted significant attention due to their intrinsic properties of large specific surface area, high chemical stability, and low skeleton density. Iron containing POPs have been synthesized by a facile one-pot aromatic electrophilic substituition reaction between pyrrole and several aromatic dialdehydes (**8**) with extended cross-linking from the macrocyclic porphyrin (**11)** repeating units through a hydrothermal reaction in the presence of small amount of $FeCl_3$ at 453 K for 3 days under acidic pH condition (**Fig. 9**).[70] This material showed good CO_2 uptake (**Table 1, entry 26-28**) attributed to stronger van der Waals force between CO_2 and the POPs surface, bearing basic porphyrin subunits in the polymeric network.[70] Triazine functionalized porphyrin-based POP-4 also showed higher CO_2 storage capacity, in a recent study [71] (**Table 1, entry 29**).

Porous nickel dopped porphyrin polymers have been synthesized by reacting 5,10,15,20-tetrakis(4-(ethynylphenyl)porphyrin (**Fig. 10**) with metal acetate in DMF.[72] The porphyrin monomer was polymerized through three types of polymerization reactions, namely Sonagashira-Hagihara coupling with tetra-iodo-phenylmethane, alkyne trimerization, and alkyne-alkyne homocoupling reactions giving polymers with a nano pore size distribution of about 0.6-1.0 nm and achieving BET surface area as high as 1711 m^2g^{-1} (**Table 1, entry 30-33**). These polymers showed exceptional adsorption capacities over 138 mgg^{-1} for carbon dioxide at 273 K and 1 bar as shown in **Fig. 11**.

High gas adsorption selectivities have also been perceived with the value up to 19 found for the CO_2/N_2 system. The heats of adsorption for CO_2 followed the tendency: ΔH **12**< ΔH **13**< ΔH **14** ≤

ΔH **15**, as shown in **Fig. 12**, being up to 29 $kJmol^{-1}$ the initial heat of adsorption estimated for CO_2. Gas adsorption selectivity of CO_2 over N_2 was calculated using the same approach used by Rosi and coworkers,[73] based on single gas sorption isotherms. The selectivity follows the sequence of Ni dopped porphyrin **12**<**13**<**14**<**15**, with values of 14.4, 15.4, 17.4 and 19.1 respectively; while the selectivity of CO_2 over CH_4 is 3.6, 3.7, 4.15, and 4.22 respectively for Ni dopped porphyrin[72] **12**, **13**, **14**, and **15**. Such gas selectivity sequences are consistent with the heat of adsorption for each material. The pronounced selectivity for CO_2 over N_2 makes this type of transition metal doped POPs good candidates for CO_2 capture and separation from the flue gas stream, where, CO_2 and N_2 amounts for around 12 mol % and 64 mol % of the total gas content, respectively. Porphyrin-based conjugated microporous polymer material with rich nitrogen sites in the skeleton, synthesized by alkyne-alkyne homocoupling reaction, display high carbon dioxide uptake capacity up to 3.58 mmol g^{-1} at 273 K and 1 bar with good selectivity towards CO_2 over N_2 and CH_4 [74] (**Table 1 entry 34**). Sonogashira-Hagihara coupling reactions have also been employed for the synthesis of porphyrinic POFs.[75] The metal center in porphyrinic POFs can be modified through post-synthetic demetallation-remetallation, which provides an opportunity to investigate the effect of the coordinatively unsaturated metal sites on gas adsorption. A study demonstrates that a demetallated por-POF-8-2H and remetallated por-POF-8-FeCl and por-POF-8-Ni exhibit similar isosteric heats of adsorption values for H_2 and CO_2, indicating the metal center has a limited impact on tuning the gas uptake capacity of porphyrinic porous materials.[75]

Polymeric materials containing imine (C=N) bonds have attracted significant attention particularly due to their ability to capture CO_2 through $N^{(\delta-)}$ - $C^{(\delta+)}O_2$ interactions.[76] Some of the POPs have enhanced gas storage values, hence the development of π-electron rich and conjugated materials with relatively high gas uptake capacities is a promising endeavor. An imine-linked porous porphyrin polymer (**Fig.13.** CuPor-BPDC-**16**), has been synthesized under solvothermal conditions *via* a Schiff base condensation reaction between 5,10,15,20-tetrakis (*p*-tetraphenyl amino) porphyrin Cu(II) and

4,4'-biphenyl dicarboxaldehyde.[77] The electron rich building blocks of CuPor-BPDC-**16**, connected by the imine bond pore walls have reactive sites for CO_2 binding. Increasing the internal molecular free pore volume by expanding the length of the building blocks could enhance the porosity for the uptake of CO_2. The CuPor-BPDC-**16** showed high CO_2 capture (5.5 wt% at 273 K and 1 bar) and very good selectivity for CO_2/CH_4 adsorption (5.6) at 1.0 bar and 273 K and exhibited a BET surface area of 442 $m^2 g^{-1}$ (**Table 1, entry 35**).

Zinc and cobalt containing two-dimensional porphyrin framework with tunable porosity has been reported.[78] The 2D solids based on various metalated TCPP (5,10,15,20-tetrakis(4-carboxyphenyl) porphyrin) present accessible metal sites with microporosity detected by CO_2 adsorption.[51] Iron(III) porphyrin based conjugated micro- and mesoporous polymer with a large surface area (1270 $m^2 g^{-1}$) and nanometer-scale pores facilitate transformation reactions.[79] FeP-CMP-**18**, synthesized by Suzuki-Miyaura cross-coupling polycondensation of iron(III)tetrakis(4'-bromophenyl)porphyrin derivative (**17**) and 1,4-phenyldiboronic acid in the presence of Pd(0) catalyst (**Fig. 14**) is a significant covalent framework which bears dense built-in catalytic sites that contains inherent nanopores that are accessible to substrates, and has large surface areas to facilitate the transformation reactions. With this design, the porphyrin polymer forms 2D frameworks with nanometer sized pore.

Nguyen's group[80] reported the synthesis of a 3D porphyrin network (Fe and Mn porphyrin porous organic polymer (**19**) by the condensation of pre-synthesized free-base porphyrin monomer and tetra-amine (**Fig. 15**). Fe(II) and Mn(II) were incorporated into the macrocycles to form metallo-porphyrin polymers with 3D pores and a moderately high surface area of 350 $m^2 g^{-1}$. Indium-based porous metal-metalloporphyrin frameworks MMPF-7 and MMPF-8 have been constructed by self-assembly of In(III) and two custom-designed porphyrin-tetracarboxylate ligands.[81] MMPF-7 and MMPF-8 exhibit CO_2 adsorption (**Table 1, entry 39,40**). Using an aluminum porphyrin as a main building block, metalloporphyrin-based conjugated microporous polymer (Al-CMP) has been synthesized solvothermally (**Fig. 16**).[82] The BET surface area has upto 839 m^2g^{-1} and a pore volume of 2.14

cm^3g^{-1}. The Al-CMP polymer has capacity to capture CO_2 4.3 wt% (or 43.12 mgg^{-1}) at 273 K and 27.43 mgg^{-1}at 298K (**Table 1, entry 41**).

3.4. Porphyrin-based crystalline materials

Generlly, there is difficulty in synthesis and purification of porpyrin-based MOF materials. To overcome this challenge we were successful in synthesizing a multiporous self organizing crystalline material by thermal crystallization, without the use of metal cations as templates. We synthesized for the first time a meso-tetra-(2-quinolyl)-porphyrin (TQP) (**Fig. 17**) from 2-quinolinecarboxaldehyde and pyrrole.[11] The resolution of the purple crystals of TQP showed that the crystal asymmetric unit of TQP comprises one half of a centrosymmetric substituted porphyrin molecule (**Fig. 18**). The unit cell contained large accessible voids, with an average volume of 423 Å perfectly adequate for CO_2 sequestering, whose volume is approximately 51 Å.[11] We found that the new multiporous crystalline framework based on meso-tetra-(2-quinolyl) porphyrin crystal channels were adequate for CO_2 reversible sequestering from 1 to 5 bar of CO_2 pressures comparing to meso-tetra-phenyl-porphyrin (TPP) (**Fig. 19**), The results showed that TQP has a high capacity to adsorb CO_2 compared to TPP, due to their free volume after packing. On the other way there is a clear interaction of CO_2 with meso-substituted nitrogen aromatic porphyrin free bases and the presence of quinoline structural motif was clearly a favourable factor in the development of crystalline molecular materials for CO_2 reversible sequestering.[11]

3.5. Porphyrin-based dendrimers

Dendrimers are repeatedly branched polymers, typically symmetric around the core, with roughly spherical three dimensional morphology and have several controllable templates to build nanoreactors. Dendritic architecture allows feasible molecular design and well-defined structure, in which the position of porphyrin and other functional groups is precisely controlled.[83-85] Dendrimer

composite membranes have been studied for carbon dioxide capture and sequestration.[86-89] Metalloporphyrin based dendrimer materials would be excellent nanoreactors for the carbon dioxide capture and storage technologies.

4. Porphyrin-based materials for CO_2 conversion

The conversion of carbon dioxide to high value chemicals has attracted much attention in the environmental and energy areas. Significant efforts have been devoted towards exploring technologies for CO_2 conversion. Different kinds of chemicals, polymers or fuels could be synthesized from CO_2 including some products that have been industrialized e.g. urea, methanol, carboxylic acids, organic carbonates and also carbamates.[90-95] Electrochemical reduction of CO_2 on various types of catalysts has been investigated intensively as a possible way to convert waste CO_2 to useful products and thus contribute to the effort to control global warming, while producing new materials. Among these catalysts, porphyrins and metalloporphyrins, acting as nanoreactors with modified size and geometries, large core sizes, a greater number of pyrrolic subunits, connectivities and linkages, and highly functionalized reactive sites are better analogues and hence stand suitable as advanced catalysts for CO_2 conversion to value added products.

The first porphyrin-based homogeneous single-site catalyst with an aluminum metal center was developed by Inoue *et al.* in 1986 (**Fig. 20**).[96] The challenging work of Wang and co-workers, who demonstrated through a series of experiments that the TPP(Co/Cl)/cocatalyst system is efficient for PO/CO_2 copolymerization,[97] which was believed to be an inactive system due to the reduced Lewis acidity of the Co center in these metalloporphyrins,[98] paved a way for advanced research in this field. Later porphyrin-based catalysts, in conjugation with nitrogen donor cocatalysts received a great scientific attention.[7] It is also believed that the porphyrin-based catalysts can have a dramatic effect in both electrochemical[99-109] and photochemical reduction of CO_2.[110,111]

Liu and coworkers have demonstrated that an effective CO_2 capture and activation is a prerequisite step for highly efficient CO_2 reduction.[112] They reported that Cu porphyrin (5,10,15,20-tetrakis(4-carboxyphenyl) porphyrin, TCPP)-based MOF enhanced the photocatalytic conversion of CO_2 to methanol compared with the samples without Cu metal. Reaction of 5,10,15,20-tetrakis(4-carboxyphenyl) porphyrin with $CuSO_4.5H_2O$ was carried in DMF solution at 100 °C for 48 h to obtain the Cu-TCPP and simultaneously a reaction without using Cu metal was carried out to obtain the TCPP (**Fig. 21**). The BET surface areas were 1187 and 932 cm^2g^{-1} for non-metallated TCPP and metallated Cu-TCPP, respectively. The smaller BET surface area of Cu-TCPP could be due to the insertion of Cu^{2+} into porphyrin, which blocks the porphyrin pores in TCPP. The pore volumes are 0.625 and 0.776 cm^3g^{-1} for Cu-TCPP and non metallated TCPP, respectively. The smaller pore volume of Cu-TCPP indicates the presence of the metal in the porphyrin ring. According to the CO_2 adsorption-desorption isotherms the amount of CO_2 adsorption capacity over Cu-TCPP is 277.4 mgg^{-1} (1 atm, 298 K) is much higher than that of non-metallated TCPP (153.1 mgg^{-1}). Very recently, isatin-porphyrin chromophore chemically bound to graphene photocatalyst-biocatalyst integrated system has been developed for highly selective methanol production from CO_2.[113] It was capable of harvesting sufficient visible light for carrying out the multi electron reduction of CO_2 to methanol at ambient conditions upon integration with the sequentially coupled enzymes.

Windle *et al.*[114] have demonstrated CO_2 reduction activity of two zinc-rhenium dyads and have compared their reactivity with that of two separate components. Dyad 1 (**23)** consists of a zinc tetraphenyl porphyrin linked to bipyridine *via* an amide spacer with the nitrogen close to the porphyrin. Dyad 2 (**24)** possesses a methoxybenzamide unit as an additional spacer, that leads to a greater porphyrin-rhenium separation (**Fig. 22**). Both dyads proved to be active photocatalysts (**Fig. 23**). In comparative studies, Dyad 2 (**24)** is more active than Dyad 1 (**23)** in terms of both TOF (Turnover Frequency) and TON (Turnover Number). In these dyads, control experiments have been conducted in the absence of CO_2 (under Ar) and in the absence of electron donor species, and in both

cases it was observed that there was no production of CO successfully. These experiments and their comparative studies between ZnTPP and ZnTPC also proved that both porphyrin and chlorin are photoactive.

Porphyrin cobalt complexes have a significant role as active catalysts in the reduction and photoreduction of CO_2 to CO.[115] The density functional theory calculations have been applied to analyse the mechanism of CO_2 reduction to CO in water, catalysed by cobalt porphyrins and it has been determined that CO_2 binds to the singly-reduced species Co(I) porphyrin.[109] Considering the trend of binuclear cobalt co-facial bis-porphyrins for electro-reduction,[116] it is surprising that these systems are used in relation to CO_2 reduction chemistry. Mixtures of cation and anion appended Co porphyrins were obtained from self-assembled cofacial bis-porphyrins in solution through Coulombic interactions[117] (**Fig. 24**).

Recently, Alenezi *et al.* have demonstrated photoelectrocatalytic conversion of CO_2 to CO with efficiency greater than 90%, on boron-doped, hydrogen terminated, *p*-type silicon electrode using a meso-tetraphenylporphyrin Fe(III) chloride (**A**) orthiolate basket porphyrin (**B**) (**Fig. 25**) in the presence of CF_3CH_2OH and 0.1 M $[NBu_4]$ $[BF_4]$/MeCN/5% DMF (v/v).[118]

Iron(0) porphyrins (**Fig. 26**) can also be used as homogeneous catalysts in a photochemical process with good performances turnover numbers in CO of up to 30 and catalytic selectivities of up to 85%.[119] Costentin et al. have demonstrated electrogenerated iron-porphyrin catalyst by introducing pendant acid group and fluorine substituents in the molecule for CO_2 to CO conversion.[120] Carbon monoxide with high catalytic selectivities (93 and 100%) and TONs of ca. 140 and 60 for photocatalytic reduction of CO_2 to CO using substituted iron(0) TPP as a homogeneous catalyst with inexpensive organic photosensitizer like fac-tris(2,2′-phenylpyridine)iridium(III) and 9-cyanoanthracene has been obtained.[121]

Metal-functionalized porphyrin-like graphene has been used for electrochemical reduction of CO_2 to CO.[107] The Co porphyrin and Fe porphyrin have been well studied for their photocatalytic and electrocatalytic activity in CO_2 reduction as homogeneous catalysts.[122,123] Porphyrin transition metal complexes have been reported as effective catalysts for CO_2 electroreduction in the form of gas diffusion electrodes, yielding CO with current efficiencies up to *ca*. 70%.[124] Recently, Matlachowski and Schwalbe developed mononuclear phenanthroline-extended metal porphyrin complexes for the photocatalytic reduction of CO_2 to CO.[125]

Cobalt porphyrin and dimethylaminopyridine system has been reported as a catalyst for the copolymerization of CO_2 and epoxide to cyclic carbonate.[126] CO_2 and epoxides can be converted to cyclic carbonates under solvent free conditions using bifunctional porphyrin catalyst Mg(II) porphyrin (**25)**, with its quaternary ammonium bromide group having high catalytic activity, high turnover number of 103000 and turnover frequency of 12000 h^{-1}.[127] By optimizing the reaction for the active catalyst (**25)** by increasing pressure of CO_2 under reflux, the yield of cyclic carbonate (**27**) was raised to 99% at 1.7 MPa CO_2 (**Fig. 27; Table 2)**. To reveal the mechanism of formation of cyclic carbonate from CO_2 and epoxide using Mg(II) porphyrin (**25**) as a catalyst, a catalytic cycle (**Fig. 28**) has been proposed. The reaction was initiated by nucleophilic attack by Br^- ion on the less-hindered side of the epoxide, along with simultaneous activation of the epoxide by coordination of the Mg(II) ion. The fact that the yield had reached a plateau in the range of 1.7-3.0 MPa CO_2 indicates that this ring-opening reaction is the rate-determining step at 1.7-3.0 MPa CO_2. The oxyanion generated from ring-opening attacks CO_2 to give a CO_2-adduct, which leads to the formation of the cyclic carbonate and regeneration of the catalyst.

Magnetic nanoparticle supported biomimetic cobalt porphyrin has been reported as an efficient and recyclable catalyst for the coupling reaction of epoxides and CO_2 to generate relevant cyclic carbonate with excellent selectivity in high yield.[128] Recently, the conversion of CO_2 and epoxides to cyclic carbonates using bifunctional porphyrin catalyst [Mg(II) porphyrin] with eight

tetraalkylammonium bromide groups having high catalytic activity, high turnover number (TON = 138000) and turnover frequency (TOF = 19000 h^{-1}) has been investigated.[129] Qin et al. have demonstrated an aluminum porphyrin complex (**Fig. 29**) with a quaternary ammonium salt co-catalyst exhibiting high activity (initial TOF = $1.85x10^5$ h^{-1}) and selectivity (>99%) for cyclic carbonate synthesis.[130] Porphyrin-based organic polymers (**Fig. 30**) as heterogeneous catalyst with TPPB, TBAB and DMAP as co-catalysts have also been used for cycloaddition of CO_2 to cyclic propylene carbonate (CPC).[131]

Metalloporphyrins show excellent catalytic activity due to dense catalytic sites covalently linked in the skeleton. Metalloporphyrin promoted cycloaddition reactions display remarkable selectivity to the cyclic carbonate without polycarbonate and other by-products. Al-CMP has been found to show good catalytic activity for cyclic carbonate synthesis with 364 h^{-1} TOF.[82] Tin(IV) porphyrin heterogeneous catalyst system has been used for synthesis of cyclic carbonates from epoxides and CO_2.[132] Manganese corrole complexes act as catalysts for copolymerization of epoxides with CO_2 affording polymeric materials.[133] [5,15-diphenylporphyrin] cobalt(III) chloride and [5-bromo-10,20-diphenyl porphyrin] cobalt(III) chloride in combination with dimethylaminopyridine are efficient catalysts for the alternating copolymerization of propylene oxide (PO) and CO_2.[134] An aluminum porphyrin complex catalyst[135] (**Fig 31**), having two para-bromine benzenes and two quaternary ammonium cations linked to benzene *via* six-methylene spacer in the mesoposition of porphyrin framework and NO_3^- as axial ligand and quaternary ammonium anion showed TOF of 560 h^{-1} at 80 ^oC and 3 MPa, yielding PPC with 94% carbonate linkage and number average molecular weight of 96 kg mol^{-1}.The PPC selectivity reached 93%, which was the highest record in this copolymerization for aluminum porphyrin complexes.

Bifunctional aluminum porphyrin complexes have been found to be highly active for the copolymerization of PO and CO_2, forming alternated poly propylene carbonate (PPC) with high molecular weight.[136] The influence of the electronic environment at the active center on the

copolymerization behavior has been studied by introducing specific substituent on the ligand framework. Catalysts bearing electron donating groups reduced the Lewis acidity of the aluminum ion, resulting in increased copolymerization rate.[136] Bifunctional aluminum porphyrin complexes as catalysts in presence of quaternary ammonium cations as cocatalysts have been designed to synthesize PPC by copolymerization of PO and CO_2. The catalytic performance was influenced by the presence of methoxy groups on the porphyrin framework as well as by the length of the alkyl chain in the quaternary ammonium cation. The optimal catalyst having six methoxy groups in the ligand framework, two trihexylammonium cations linked to benzene *via* a six-methylene spacer, and NO^{3-} as the axial ligand and quaternary ammonium anions exhibited a TOF of 1320 h^{-1} with 93% PPC selectivity at 80 °C and 3 MPa within 5 h, which was the highest recorded in this copolymerization of aluminum porphyrin complexes.[137]

Homogeneous catalysts discussed above, however, have difficulty in recovery and reuse. In this persuit immobilization of bifunctional catalyst on biogenous iron oxide (BIO) (produced by iron-oxidizing bacteria, Leptothrixochracea) has been reported to give a highly active and recyclable heterogeneous catalyst for the synthesis of cyclic carbonates **27** from epoxides **26** and CO_2 (**Fig. 27**). Zn(II) porphyrin linked to BIO *via* four tetraalkylammonium bromide groups (**Fig. 32**) functions as a nanoreactor and possesses high catalytic activity and reusability at a catalyst loading of 0.1 mol%, after nine times reuse with 99% yield. Zn(II) porphyrin BIO showed higher recyclability than Mg(II) porphyrin BIO due to the higher stability of Zn(II) porphyrin as compared with Mg(II) porphyrin.[138]

Porphyrin cobalt(III) chloride complexes have been synthesized and studied for their reactivity towards PO/CO_2 coupling or copolymerization.[139] The activity and selectivity of these cobalt-porphyrins are strongly dependent on the substitution pattern of the ligand framework and enables tailoring of the product selectivity; electron withdrawing substituents afford exclusive cyclization (forming cyclic carbonate) while electron donating fragments afford highly active copolymerization catalysts, producing polycarbonate with excellent properties. While the nitro substituted complex

(**28**), in combination with an onium salt, shows moderate activity towards cyclization, the onium systems show superior copolymerization activity in comparison to tetraphenyl porphyrin Co(III) chloride with high selectivity and conversion to PPC (**31**) (**Fig. 33**). Complexes bearing longer alkoxy-substituents demonstrate highest polymerization activity and molecular weights, however all substituted catalyst systems display a reduced tolerance to increased temperature with respect to PPC formation. Cobalt porphyrin complex has also been used in combination with ionic organic ammonium salt for the region-specific copolymerization of PO and CO_2.[140] The reactivity of porphyrin- and salen-M(III) cations, where M = Al, Ga, Cr, and Co, metal complexes have been reported in ring-opening polymerizations and copolymerizations with PO and CO_2, respectively.[98]

Cobalt bis-porphyrins along with a mono-nuclear cobalt porphyrin have been synthesized and used as catalysts for carbon dioxide-propylene oxide copolymerization, showing that the copolymerization was effective in the presence of bis(triphenylphosphoranyl) ammonium chloride cocatalyst.[141] The catalytic activities of the mononuclear (**32**) and bis-para-tethered cobalt bis-porphyrin (**33**) (**Fig. 34**) are largely comparable with selective formation of PPC (**31**), showing no benefit of dinuclearity in contrast to the case of cobalt salen complexes. This suggests that polymer growth has its origin exclusively from one metal centre. The bis-ortho-tethered porphyrin demonstrated considerably reduced activity by forming dominantly CPC (**30**). Time-resolved UV/Vis spectroscopic studies suggested a general intolerance of the cobalt(III) porphyrin catalysts towards the copolymerization conditions in the absence of carbon dioxide pressure, leading to catalytically inactive cobalt(II) species. In the presence of carbon dioxide, the bis-ortho-tethered catalyst showed the fastest deactivation. Recently, Xia et al. have demonstrated a deactivation of cobalt(III)-based porphyrin and salen catalysts via reduction to cobalt(II) species in the copolymerization of PO and CO_2.[142]

Chatterjee and Chisholm[143,144] studied the reactivities of TPP (**34**), 5,10,15,20-tetrakis(pentafluorophenyl)porphyrin (TFPP) (**35**), 2,3,7,8,12,13,17,18-octaethyl porphyirn (OEP) (**36**) based aluminumand chromium complexes with respect to their ability to homopolymerize PO

and copolymerize PO and CO_2 into polypropylene oxide (PPO) and PPC **31**, respectively, with and without the presence of a co-catalyst (4-dimethylaminopyridine or a PPN^+ salt, where the anion is Cl^- or N_3^-). In the presence of a co-catalyst, the TFPP complex was most active in copolymerization to yield PPC. An increase in the PPN^+ X^-/[Al] ratio decreased the rate of PPC formation and favored the formation of propylene carbonate, (PC) (**30) Fig. 35**. Manganese-corrole complexes in combination with a co-catalyst [PPN]X ($[PPN]^+$ bis(triphenylphosphoranylidene) iminium have been found to be new versatile catalysts for the copolymerization of epoxides with CO_2 to form polycarbonates[145] **(31**).

Self-assembly as a burgeoning section of supramolecular chemistry has been a prolific tool for the construction of diverse fascinating hollow 3D structures. Self-assembly of the octatopic porphyrin ligand of tetrakis(3,5-dicarboxybiphenyl) porphyrin with the *in situ* generated $Cu_2(CO_2)_4$ paddle wheel moieties afforded a porous metal-metalloporphyrin framework.[146] MMPF-9 which features a high density of Cu(II) sites confined within nanoscopic channels demonstrated excellent performances as a heterogeneous Lewis-acid catalyst for chemical fixation of CO_2 to form cyclic carbonates (**30**) at room temperature under 1 atm pressure.

Feng *et al*. have assembled highly stable and highest BET surface area (2600 m^2g^{-1}) of porphyrin Zr MOFs with 3D porous coordination network through a linker-elimination.[147] The cobalt porphyrin zirconium MOF, PCN-224 (Co) as an efficient and recyclable catalyst for the coupling reaction of epoxides and CO_2 to formation of cyclic carbonate **(30**) (**Fig. 36**). In a typical reaction, an autoclave reactor was added PCN-224(Co) (32.1 μmol), tetrabutylammoniumchloride (71.6 μmol) and PO (35.7 mmol) and the reactor was pressurized to 2 MPa with CO_2 and temperature was maintained at 100 °C for 4 h. At end of the reaction, PCN-224(Co) was recovered and reused.[147]

A porous metal-metalloporphyrin framework, MMPF-9, has been synthesized using a custom-designed octatopic porphyrin ligand that links $Cu_2(CO_2)_4$ paddlewheel moieties. MMPF-9 has a high density of copper sites in the nanoscopic channels, demonstrating it to be a highly efficient Lewis

acid based heterogeneous catalyst for chemical fixation of CO_2 with epoxides to form cyclic carbonates under ambient conditions.[148] Mechanistic studies estimate that the epoxide first binds with the Lewis acidic copper site in the nanoreactor of MMPF-9 through the oxygen atom of epoxide, and leads to the activation of the epoxy ring. The less-hindered carbon atom of the activated epoxide is then attacked by the Br^- generated from n-Bu_4NBr to open the epoxy ring. Subsequently CO_2 interacts with the oxygen anion of the opened epoxy ring to form an alkylcarbonate anion, which is then converted into the corresponding cyclic carbonate through a ring closing. It has been speculated that a high density of copper Lewis acid sites pointing toward the channel center could boost the synergistic effect using n-Bu_4NBr thus facilitating the cycloaddition reaction, which thereby results in high catalytic activity of MMPF-9 for converting CO_2 into cyclic carbonates under ambient conditions.[148]

Mechanistic studies to estimate the catalytic activity for (1) PPC, (2) PPC/CPC selectivity, and (3) PPC/PPO selectivity for metal catalyzed (metal complexes, including metalloporphyrins) copolymerization of PO with carbon dioxide has been conducted to propose some indicators to rationalize catalytic activities.[149] Using DFT, Gibbs energies of the key intermediates in the copolymerization have been calculated and correlation between the relative Gibbs energy and (1) catalytic activity for PPC generation, (2) PPC/CPC selectivity, and (3) PPC/PPO selectivity have afforded an effective indicator, ΔG_{crb}-ΔG_{epx}, for the evaluation of the catalytic activities for PPC generation. Furthermore, the ΔG_{epx} itself was found to be an indicator for PPC/CPC selectivity. If ΔG_{epx} is too small, the complex tends to be CPC selective. These indicators can be easily calculated by DFT methods without computing transition states, so that it can be used as a standard when the brand-new catalyst candidates are screened. An indicator, ΔG_{alk}-ΔG_{epx}, and steric environment around the active center determined the PPC/PPO selectivity. Small ΔG_{alk}-ΔG_{epx} and small steric bulk around the metal center facilitate the PPO formation, which resulted in lowering PPC/PPO selectivity. This is a general explanation for catalytic activity and selectivities common for versatile

metal complexes and we anticipate that the next 10 years of research will focus more closely on the applications of nanoreactor based materials for CO_2 conversion.

Graphene based photocatalyst covalently bonded with anthraquinone substituted porphyrin has been used for the artificial photosynthesis system for an efficient photosynthetic production of formic acid from carbondioxide.[150] Porphyrin and phthalocyanine adsorbed Nafion membranes have also been used for the photocatalytic reduction of carbon dioxide to formic acid.[151] Porphyrin and graphene composites as photocatalyst for conversion of CO_2 to CH_4 and acetylene under visible light have been used for the first time, opening new vistas in the field of CO_2 capture and conversion technology.[152]

5. Conclusions

The field of porphyrin- and metalloporphyrin-based nanoreactors for CO_2 capture and conversion is still in its budding stage, with only a limited number of reports having appeared that deal with the chemistry and its applications in CO_2 capture and conversion to value added chemicals. However, the field is abound with opportunities and is bound to advance. Porphyrins with their inherent catalytic properties, have the potential to be used as promising catalysts for the chemical conversion of CO_2 more selectively and at the same time their uniqueness of structure could be utilized to modelate the pore dimensions of the designed framework, necessary for CO_2 adsorption. We believe that this review provides guidance to design the best porphyrin based nanoreactors as COFs, MOFs, dyads, dimmers or porous materials which would be promising tools to overcome the existing challenges for solving all problems related to implementation of effective CO_2 capture and sustainable CO_2 conversion technologies.

Acknowledgments

The authors gratefully acknowledge Fundação para a Ciência e a Tecnologia (FCT), Portugal, for financial support troutgh the project FCT/COMPETE PTDC/AAC-CLI/118092/2010 coordinated by Prof. Abilio Sobral. The authors also acknowledge FCT for the postdoctoral fellowships to Dr. S. Kumar (SFRH/BPD/86507/2012), Dr. M.Y. Wani (SFRH/BPD/86581/2012), Drª. Joana de A. e Silva (SFRH/BD/61637/2009) and Drª. Claudia Arranja (SFRH/BD/48269/2008).

Abbreviations

BIO Biogenous iron oxide; **BET** Brunauer-Emmet-Teller; **CO_2** Carbondioxide; **CCC** Carbon capture and conversion; **CCS** Carbon capture and storage; **CH_4** Methane; **CO** Carbon monoxide; **CPC** cyclic propylene carbonate; **CRF** Confined Reaction Fields; **COF** Covalent-organic framework; **MOF** Metal-organic framework; **MOM** Metal-organic material; **MMPF** Metal-metalloporphyrin framework; **OEP**2 ,3,7,8,12,13,17,18-octaethylporphyirn; **PCN** Porous coordination network; **POP** Porous organic polymer; **POF** Porous organic framework; **PPO** Polypropylene oxide; **PPC** Polypropylene carbonate; **Por** Porphyrin; **SBU** symmetric secondary building unit; **TQP** meso-tetra-(2-quinolyl)-porphyrin; **TPP** meso-tetra-phenyl-porphyrin; **TCPP** 5,10,15,20-tetrakis(4-carboxyphenyl) porphyrin; **TOF** Turnover frequency; **TON** Turnover number; **TFPP** 5,10,15,20-tetrakis(pentafluorophenyl) porphyrin; **UNLPF** University of Nebraska-Lincoln porous framework.

References

1 The International Energy Outlook (IEO2014); U.S. Energy Information Administration (EIA) 2014, http://www.eia.gov/forecasts/ieo/

2 R. S. Haszeldine, Science 2009, 325, 1647-1652.

3 X. Xu, C. Song, J. M. Andresen, B. G. Miller and A. W. Scaroni, Micropor. Mesopor. Mat., 2003, 62, 29-45.

4 D. M. D'Alessandro, B. Smit, and J. R. Long, Angew. Chem. Int. Ed., 2010, 49, 6058 – 6082.

5 K. Sumida, D. L. Rogow, J. A. Mason, T. M. McDonald, E. D. Bloch, Z. R. Herm, T. H. Bae and J. R. Long, Chem. Rev., 2012, 112, 724-781.

6 D. M. D Alessandro, B. Smit and J. R. Long, Angew. Chem. Int. Ed., 2010, 49, 6058-6082.

7 S. Klaus, M. W. Lehenmeier, C. E. Anderson and B. Rieger, Coord. Chem. Rev., 2011, 255, 1460-1479.

8 C. C. Wang, Y. Q. Zhang, J. Li and P. Wang, J. Molecul. Struct., 2015, 1083,127-136.

9 S. Klaus, M. W. Lehenmeier, C. E. Anderson and B. Rieger Coord. Chem. Rev., 2011, 255, 1460-1479.

10 S. Kumar, J. A. e Silva, M. Y. Wani, C. M. F. Dias and A. J. F. N. Sobral, J. Disper. Sci. Technol., 2015, DOI: 10.1080/01932691.2015.1035388.

11 J. A. Silva, V. F. Domingos, D. Marto, L. D. Costa, M. Marcos, M. R. Silva, J. M. Gil and A. J. F. N. Tet. Lett., 2013, 54, 2449-2451.

12 A. J. F. N. Sobral, L. L. G. Justino, A. C. C. Santos, J. A. Silva, C. T. Arranja, M. R. Silva and A. M. Beja, J. Porphyrins Phthalocyanines, 2008, 12, 845-848.

13 A. J. F. N. Sobral, S. M. Melo, M. L. Ramos, R. Teixeira, S. M. Andrade and S. M. B. Costa, Tet. Lett., 2007, 48, 3145-3149.

14 S. Costa, A. G. Silva, A. J. F. N. Sobral and D. M. Togashi, Phys. Chem. Chem. Phys., 2005, 7, 3874-3883.

15 S. M. Andrade, R. Teixeira, S. M. B. Costa, A. J. F. N. Sobral, Biophys. Chem., 2008, 133, 1-10.

16 G. A. Rance, W. A. Solomonsz and A. N. Khlobystov, Chem. Commun., 2013,49, 1067-1069.

17 R. Johnson, Nature Chem., 2014, 6, 5, doi:10.1038/nchem.1840.

18 A. N. Khlobystov, ACS Nano, 2011, 5, 9306-9312.

19 Z. Q. Li, Y. M. Zhang, Y. Chen and Y. Liu, Chem. Eur. J., 2014, 20, 8566-8570.

20 Y. C. Chen, Q. Wang and A. Ostafin Introduction to nanoreactor technology. In: A. Ostafin, and K. Landfester, editors. Nanoreactor Engineering for Life Sciences and Medicine, Norwood: Arthech House; 2009, 1-131.

21 D. M. Vriezema, M. C. Aragones, J. A. A. W. Elemans, J. J. L. M. Comelissen, A. E. Rowan and R. J. M. Nolte, Chem. Rev., 2005,105,1445-1489.

22 A. D'Urso, M. E. Fragala and R. Purrello. Chem. Commun., 2012, 48, 8165-8176.

23 V. Pillai, P. Kumar, M. J. Hou, P. Ayyub and D. O. Shah, Adv. Colloid. Interfac. Sci., 1995, 55, 241-269.

24 M. A. Malik, M. Y. Wani and M. A. Hashim, Arab. J. Chem., 2012, 5, 397-417.

25 T. H. Tran-Thi, R. Dagnelie, S. Crunaire and L. Nicole, Chem. Soc. Rev., 2011, 40, 621–639.

26 C. G. Palivan, O. F. Onaca, M. Delcea, F. Itel and W.Meier, Chem. Soc. Rev. 2012, 41, 2800-2823.

27 M. Grzelakowski, O. Onaca, P. Rigler, M. Kumar and W.Meier, Small, 2009, 5, 2545-2548.

28 Y. M. Mohan, K. Lee, T. Premkumar and K. E. Geckeler, Polymer, 2007, 48, 158-164.

29 K. Landfester and A. Musyanovych, Adv. Polym. Sci., 2010, 234, 39-63.

30 M. Remskar, A. Mrzel, M. Virsek and A. Jesih, Adv. Mater., 2007, 19, 4276-4278.

31 S. Ding, J. S. Chen, G. Qi, X. Duan, Z. Wang, E. P. Giannelis, L. A. Archer and X. W. Lou, J. Am. Chem. Soc., 2011, 133, 21-23.

32 Y. liu, Y. Wang, Y. Wang, J. Lu, V. Pinon and M. Weck, J. Am. Chem. Soc., 2011, 133, 14260-14263.

33 M. C. Aragones, H. Engelkamp, V. I. Claessen, N. A. J. M. Sommerdijk, A. E. Rowan, P. C. M. Christianen, J. C. Maan, B. J. M. Verduin, J. J. L. M. Cornelissen and R. J. M. Nolte. Nature Nanotech., 2007, 2, 635-639.

34 W. Zhao and Q. Zhong, J. Incl. Phenom. Macrocycl. Chem., 2012, 72, 1-14.

35 S. Polarz and A. Kuschel, Chem. Eur. J., 2008, 14, 9816-9829.

36 K. S. W. Sing, D. H. Everett, R. A. W. Haul, L. Moscou, R. A. Pierotti, J. RouquQrol and T. Siemieniewska, Pure Appl. Chem., 1985, 57, 603-619.

37 D. G. Shchukin, and G. B. Sukhorukov, Advanced Materials., 2004, 16, 671-682.

38 Y. Wu, G. Cheng, K. Katsov, S. W. Sides, J. Wang, J. Tang, G. H. Fredrickson, M. Moskovits and G. D. Stucky, Nature Mat., 2004, 3, 816-822.

39 C. H. Yu, C. H. Huang and C. S. Tan, Aerosol Air Qual. Res., 2012, 12, 745-769.

40 A. R. Millward and O. M. Yaghi, J. Am. Chem. Soc., 2005, 127, 17998-17999.

41 H. Furukawa, K. E. Cordova, M. O'Keeffe and O. M. Yaghi, Science, 2013, 341, 1230444-1-1230444-12.

42 W. Y. Gao, M. Chrzanowski and S. Ma, Chem. Soc. Rev., 2014, 43, 5841-5866.

43 G. Ferey, C. Serre, T. Devic, G. Maurin, H. Jobic, P. Llewellyn, G. D. Weireld, A. Vimont, M. Daturif and J. S. Chang, Chem. Soc. Rev., 2011, 40, 550-562.

44 J. Liu, P. K. Thallapally, B. P. McGrail, D. R. Brown and J. Liu, Chem. Soc. Rev. 2012, 41, 2308-2322 .

45 J. An and N. L. Rosi, J. Am. Chem. Soc., 2010, 132, 5578-5579.

46 J. R. Li, Y. Ma, M. C. McCarthy, J. Sculley, J. Yu, H. K. Jeong , P. B. Balbuena , H.C. Zhou, Coord. Chem. Rev., 2011, 255, 1791-1823.

47 K. Sumida, D. L. Rogow, J. A. Mason, T. M. McDonald, E. D. Bloch, Z. R. Herm, T. H. Bae and J. R. Long, Chem. Rev., 2012, 112, 724-781.

48 J. A. Johnson, S. Chen, T. C. Reeson, Y. S. Chen, X. C. Zeng and J. Zhang, Chem. Eur. J., 2014,

20, 7632-7637

49 G. Nandi and I. Goldberg, Chem. Commun., 2014, 50, 13612-13615.

50 F. Gao, J. B. Zhang, C. P. Li, T. R. Huo and X. H. Wei, Chin. Chem. Lett., 2013, 24, 249-252.

51 H. C. Kim, Y. S. Lee, S. Huh, S. J. Lee and Y. Kim, Dalton Trans., 2014, 43, 5680-5686.

52 O. K. Farha, A. M. Shultz, A. A. Sarjeant, S. T. Nguyen and J. T. J. Hupp, J. Am. Chem. Soc., 2011, 133, 5652–5655.

53 X. S. Wang, L. Meng, Q. Cheng, C. Kim, L. Wojtas, M. Chrzanowski, Y. S. Chen, X. P. Zhang, and S. Ma, J. Am. Chem. Soc. 2011, 133, 16322-16325.

54 X. S. Wang, M. Chrzanowski, C. Kim, W. Y. Gao, L. Wojtas, Y. S. Chen, X. P. Zhang and S. Ma, Chem. Commun., 2012, 48, 7173-7175.

55 X. S. Wang, M. Chrzanowski, W. Y. Gao, L. Wojtas, Y. S. Chen, M. J. Zaworotko and S. Ma, Chem. Sci., 2012, 3, 2823-2827.

56 S. Y. Ding and W. Wang, Chem. Soc. Rev., 2013, 42, 548-568.

57 K. T. Jackson, T. E. Reich and H. M.. El-Kaderi, Chem. Commun. 2012, 48, 8823-8825.

58 Z. Li, X. Feng, Y. Zou, Y. Zhang, H. Xi, X. Liu and Y. Mu, Chem. Commun., 2014, 50, 13825-13828.

59 P. Kuhn, M. Antonietti and A. Thomas, Angew. Chem. Int. Ed., 2008, 47, 3450-3453.

60 S. Kandambeth, D. B. Shinde, M. K. Panda, B. Lukose, T. Heine and R. Banerjee, Angew. Chem. Int. Ed., 2013, 52, 13052-13056.

61 D. N. Bunck and W. R. Dichtel, J. Am. Chem. Soc., 2013, 135, 14952-14955.

62 A. P. Cote, A. I. Benin, N. W. Ockwig, M. O'Keeffe, A. J. Matzger and O. M.. Yaghi, Science, 2005, 310, 1166-1170.

63 H. M. El-kaderi, J. R. Hunt,. J. L. Mendoza-Cartes, A. P. Cote, R. E. Taylor, M. O'Keeffe and O. M. Yaghi, Science, 2007, 316, 268-272.

64 H. Furukawa and O. M. Yaghi, J. Am. Chem. Soc., 2009, 131, 8875-8883.

65 A. Phan, C. J. Doonan, F. J. Uribe-Romo, C. B. Knobler, M. O'Keeffe and O. M.Yaghi, Accounts Chem. Res. 2010, 43, 58-67.

66 X. Feng, X. Ding and D. Jiang, Chem. Soc. Rev., 2012, 41, 6010-6022.

67 X. Feng, L. Liu, Y. Honsho, A. Saeki, S. Seki, S. Irle, Y. Dong, A. Nagai and D. Jiang, Angew. Chem. Int. Ed., 2012, 51, 2618-2622.

68 S. Wan, F. Gandara, A. Asano, H. Furukawa, A. Saeki, S. K. Dey, L. Liao, M. W. Ambrogio, Y. Y. Botros, X. Duan, S. Seki, J. F. Stoddart and O. M.Yaghi, Chem. Mater. 2011, 23, 4094-4097.

69 N. Huang, R. Krishna, and D. Jiang, J. Am. Chem. Soc. 2015, 137, 7079-7082.

70 A. Modak, M. Nandi, J. Mondal and A.Bhaumik, Chem. Commun. 2012, 48, 248-250.

71 A. Modak, M. Pramanik, S. Inagaki and A. Bhaumik, J. Mater. Chem. A, 2014, 2, 11642-11650.

72 Z. Wang, S. Yuan, A. Mason, B. Reprogle, D. J. Liu and L. Yu, Macromolecules, 2012, 45, 7413-7419.

73 J. An, S. J. Geib and N. L. Rosi, J. Am. Chem. Soc., 2010, 132, 38-39.

74 X. Liu, A. Sigen, Y. Zhang, X. Luo, H. Xia, H. Li and Y. Mu, RSC Adv, 2014, 4, 6447-6453.

75 Q. Lin, J. Lu, Z. Yang, X. C. Zeng, J. Zhang, J. Mater. Chem. A, 2014, 2, 14876-14882.

76 S. Yang, J. Sun, A. J. Ramirez-Cuesta, S. K. Callear, W. I. F. David, D. P. Anderson, R. Newby, A. J. Blake, J. E. Parker, C. C. Tang and M. Schroder, Nat. Chem. 2012, 4, 887-894.

77 V. S. P. K. Neti, X. Wu, S. Deng and L.Echegoyen, Polym. Chem., 2013, 4, 4566-4569.

78 E. Y. Choi, C. A. Wray, C. Hu and W.Choe, CrystEngComm., 2009, 11, 553–555.

79 L. Chen, Y. Yang and D.Jiang, J. Am. Chem. Soc., 2010, 132, 9138-9143.

80 A. M. Shultz, O. K. Farha, J. T. Hupp and S. T. Nguyen, Chem. Sci., 2011, 2, 686-689.

81 W. Y. Gao, Z. Zhang, L. Cash, L. Wojtas, Y. S. Chen and S. Ma, Cryst. Eng. Comm. 2013, 15, 9320-9323.

82 X. Sheng, H. Guo, Y. Qin, X. Wang and F. Wang, RSC Adv., 2015, 5, 31664-31669.

83 D. Astruc, Nature Chem., 2012, 4, 255-267.

84 S. Y. Lim and E. J. Shin, Bull. Korean Chem. Soc., 2008, 29, 1353-1358.

85 P. J. Dandliker, F. Diederich, M. Gross, C. B. Knobler, A. Louati and E. M. Sanford, Angew. Chem. Int. Ed., 1994, 33, 1739-1742.

86 S. Duan, I. Taniguchi, T. Kai and S. Kazama, J. Membrane Sci., 2012, 423–424, 107-112.

87 I. Taniguchi, S. Duan, S. Kazama and Y. Fujioka, J. Membrane Sci., 2008, 322, 277-280.

88 T. Kai, T. Kouketsu, S. Duan, S. Kazama and K. Yamada, Sep. Purif. Technol., 2008, 63, 524-530.

89 B. Yu, H. Cong, X. Zhao, Song and Z. Chen, Adsorp. Sci. Technol., 2011, 29, 781-788.

90 M. Mikkelsen, M. Jorgensen and F. C. Krebs, Energy Environ. Sci., 2010, 3, 43-81.

91 T. Sakakura, J. C. Choi and H.Yasuda, Chem. Rev., 2007, 107, 2365-2387.

92 T. Sakakura and K. Kohno, Chem. Commun., 2009, 1312-1330.

93 D. J. Darensbourg, Chem. Rev., 2007, 107, 2388-2410.

94 A. J. Morris, G. J. Meyer and E. Fujita, Accounts Chem. Res., 2009, 42, 1983-1994.

95 C. Wu, J. Wang, P. Chang, H. Cheng, Y. Yu, Z. Wu, D. Dong and F. Zhao, Phys. Chem. Chem. Phys., 2012, 14, 464-468.

96 T. Aida, M. Ishikawa and S. Inoue, Macromolecules, 1986, 19, 8-13.

97 Y. Qin, X. Wang, S. Zhang, X. Zhao and F. Wang, J. Polym. Sci. Part A, 2008, 46, 5959-5967.

98 P. Chen, M. H. Chisholm, J. C. Gallucci, X. Zhang and Z. Zhou, Inorg. Chem., 2005, 44, 2588-2595.

99 I. Bhugun, D. Lexa and J. M. Saveant, J. Am. Chem. Soc., 1994, 116, 5015-5016.

100 C. Costentin, S. Drouet, M. Robert and J. M. Saveant, J. Am. Chem. Soc., 2012, 134, 11235-11242.

101 C. Costentin, S. Drouet, G. Passard, M. Robert, J. M. Savéant, J. Am. Chem. Soc. 2013, 135, 9023-9031.

102 C. Costentin, S. Drouet, M. Robert and J. M. Saveant, Science, 2012, 338, 90-94.

103 G. Ramirez, G. Ferraudi, Y. Y. Chen, E. Trollund and D. Villagra, Inorg. Chim. Acta, 2009, 362,

5-10.

104 Y. I.Ogur, J. Mol. Catal., 1988, 47, 51-57.

105 I. Bhugun, D. Lexa and J. M. Saveant, J. Phys. Chem., 1996, 100, 19981-19985.

106 I. Bhugun, D. Lexa and J. M. Saveant, J. Am. Chem. Soc., 1996, 118, 1769-1776.

107 V. Tripkovic, M. Vanin, M. Karamad, M. E. Bjorketun, K. W. Jacobsen, K. S. Thygesen and J. Rossmeis, J. Phys. Chem., C 2013, 117, 9187-9195.

108 I. M. B. Nielsen and K. Leung, J. Phys. Chem., A 2010, 114, 10166-10173.

109 K. Leung, I. M. B. Nielsen, N. Sal, C. Medforth, J. A. Shelnutt, J. Phys. Chem., A 2010, 114, 10174-10184.

110 J. Grodkowski and P. Neta, J. Phys. Chem., A 2000, 104, 4475-4479.

111 T. Dhanasekaran, J. Grodkowski, P. Neta, P. Hambright, E. Fujita, J. Phys. Chem., A 1999, 103, 7742-7748.

112 Y. Liu, Y. Yang, Q. Sun, Z. Wang, B. Huang, Y. Dai, X. Qin and X. Zhang, ACS Appl. Mater. Interfaces, 2013, 5, 7654-7658.

113 R. K. Yadav, G. H. Oh, N. J. Park, A. Kumar, K. Kong and J. O. Baeg, J. Am. Chem. Soc., 2014, 136, 16728-16731.

114 C. D. Windle, M. V. Campian, A. K. D. Klair, E. A. Gibson, R. N. Perutz and J. Schneider, Chem. Commun., 2012, 48, 8189-8191.

115 J. M. Saveant, Chem. Rev., 2008, 108, 2348-2378.

116 J. Rosenthal and D. G. Nocera, Prog. Inorg. Chem., 2007, 55, 483-544.

117 O. Enoki, T. Imaoka and K. Yamamoto, Macromol. Symp., 2003, 204, 151-158.

118 K. Alenezi, S. K. Ibrahim, P. Li and C. J. Pickett, Chem. Eur. J., 2013, 19, 13522-13527.

119 J. Bonin, M. Chaussemier, M. Robert and M. Routier, ChemCatChem, 2014, 6, 3200-3207.

120 C. Costentin, G. Passard, M. Robert and J. M. Savéant, Proc. Natl. Acad. Sci. USA, 2014, 111, 14990-14994.

121 J. Bonin, M. Robert and M..Routier, J. Am. Chem. Soc., 2014, 136, 16768-16771.

122 D. Behar, T. Dhanasekaran, P. Neta,. C. M. Hosten, D. Ejeh, P. Hambright and E. Fujita, J. Phys. Chem., A 1998, 102, 2870-2877.

123 J. Grodkowski, D. Behar, P. Neta and P. Hambright, J. Phys. Chem., A 1997, 101, 248-254.

124 T. V. Magdesieva, T. Yamamoto, D. A. Tryk and A. Fujishima, J. Electrochem. Soc., 2002, 149, D89-D95.

125 C. Matlachowski and M. Schwalbe, Dalton Trans., 2015, 44, 6480-6489.

126 H. Sugimoto and K. Kuroda, Macromolecules, 2008, 41, 312-317.

127 T. Ema, Y. Miyazaki, S. Koyama, Y. Yano and T. Sakai, Chem. Commun., 2012, 48, 4489-4491.

128 D. Bai, Q. Wang, Y. Song, B. Li and H. Jing, Catalysis Commun., 2011, 12, 684–688.

129 T. Ema, Y. Miyazaki, J. Shimonishi, C. Maeda and J. Hasegawa, J. Am. Chem. Soc., 2014, 136, 15270-15279.

130 Y. Qin, H. Guo, X. Sheng, X. Wang and F. Wang, Green Chem., 2015, 17, 2853-2858.

131 A. Chen, Y. Zhang, J. Chen, L. Chen and Y. Yu, J. Mater. Chem. A, 2015, 3, 9807-9816.

132 F. Zadehahmadi, F. Ahmadi, S. Tangestaninejad, M. Moghadam, V. Mirkhani, I. M. Baltork and R. Kardanpour, J. Mol. Catal. A: Chem., 2015, 398, 1-10.

133 C. Robert, T. Ohkawara and K. Nozak, Chem. Eur. J., 2014, 20, 4789-4795.

134 X. Jiang, F. Gou and H. Jing, J. Catal., 2014, 313, 159-167.

135 X. Sheng, Y. Wang, Y. Qin, X. Wang and F. Wang, RSC Adv., 2014,4, 54043-54050.

136 W. Wu, X. Sheng, Y. Qin, L. Qiao, Y. Miao, X. Wang and Fosong Wang, J. Polym. Sci., Part A: Polym. Chem., 2014, 52, 2346-2355.

137 X. Sheng, W. Wu, Y. Qin, X. Wang and F. Wang, Polym. Chem., 2015,6, 4719-4724.

138 T. Ema, Y. Miyazaki, T. Taniguchi and J. Takada, Green Chem., 2013, 15, 2485-2492.

139 C. E. Anderson, S. I. Vagin, W. Xia, H. Jin and B. Rieger, Macromolecules, 2012, 45, 6840−6849.

140 Y. Qin, X. Wang, S. Zhang, X. Zhao and F.Wang, J. Polym. Sci. Part A Polym. Chem., 2008, 46, 5959-5967.

141 C. E. Anderson, S. I. Vagin, M. Hammann, L. Zimmermann and B. Rieger, ChemCatChem, 2013, 5, 3269-3280.

142 W. Xia, K. A. Salmeia, S. I. Vagin and B. Rieger, Chem. Eur. J., 2015, 21, 4384-4390.

143 C. Chatterjee and M. H. Chisholm, Inorg. Chem., 2011, 50, 4481-4492.

144 C. Chatterjee and M. H. Chisholm, Inorg. Chem., 2012, 51, 12041-12052.

145 C. Robert, T. Ohkawara and K. Nozaki, Chem. Eur. J., 2014, 20, 4789-4795.

146 W. Y. Gao, L. Wojtas and S. Ma, Chem. Commun., 2014, 50, 5316-5318.

147 D. Feng, W. C. Chung, Z. Wei, Z. Y. Gu, H. L. Jiang, Y. P. Chen, D. J. Darensbourg and H. C. Zhou, J. Am. Chem. Soc., 2013, 135, 17105-17110.

148 W. Y. Gao, L. Wojtas and S. Ma, Chem. Commun., 2014, 50, 5316-5318.

149 T. Ohkawara, K. Suzuki, K. Nakano, S. Mori and K. Nozaki, J. Am. Chem. Soc., 2014, 136, 10728-10735.

150 R. K. Yadav, J. O. Baeg, G. H. Oh, N. J. Park, K. Kong, J. Kim, D. W. Hwang and S. K. Biswas, J. Am. Chem. Soc., 2012, 134, 11455-11461.

151 J. Premkumar and P. Ramaraj, J. Phochem. Photobio. A: Chem., l997, 110, 53-58.

152 Tongshun Wu, Luyi Zou, Dongxue Han, Fenghua Li, Qixian Zhang and Li Niu, Green Chem., 2014, 16, 2142-2146.

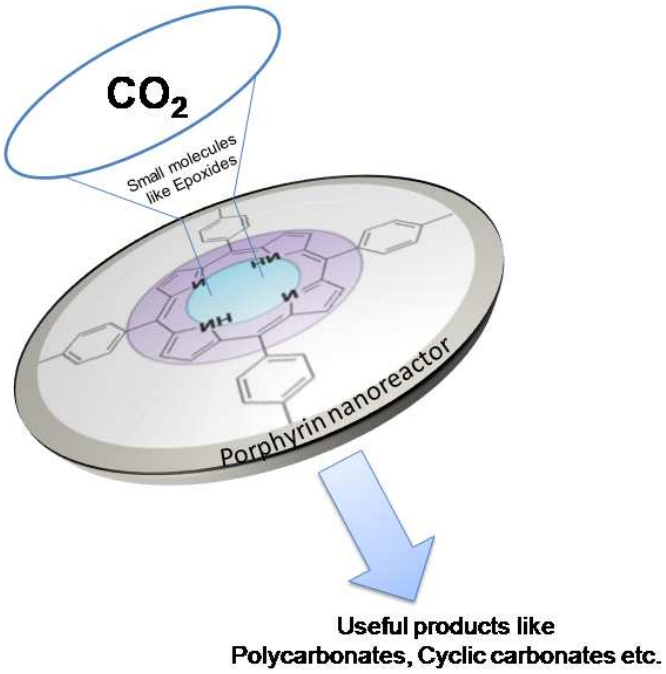

Fig. 1 Porphyrins based nanoreactors in CO_2 conversion: a pictoral description.

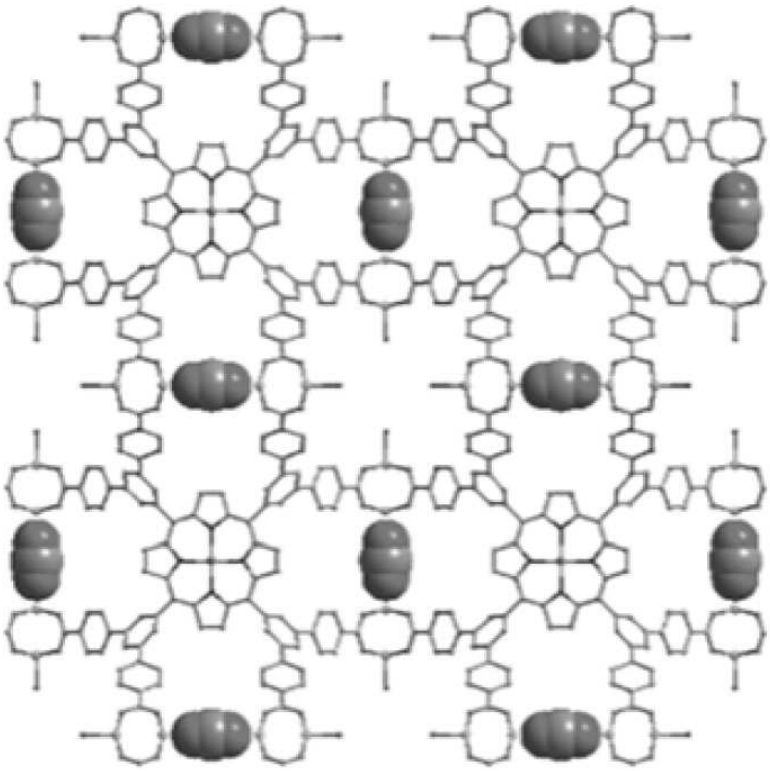

Fig. 2 X-ray crystallographic structure of porphyrinic MOF (UNLPF-2) (with permission).[48]

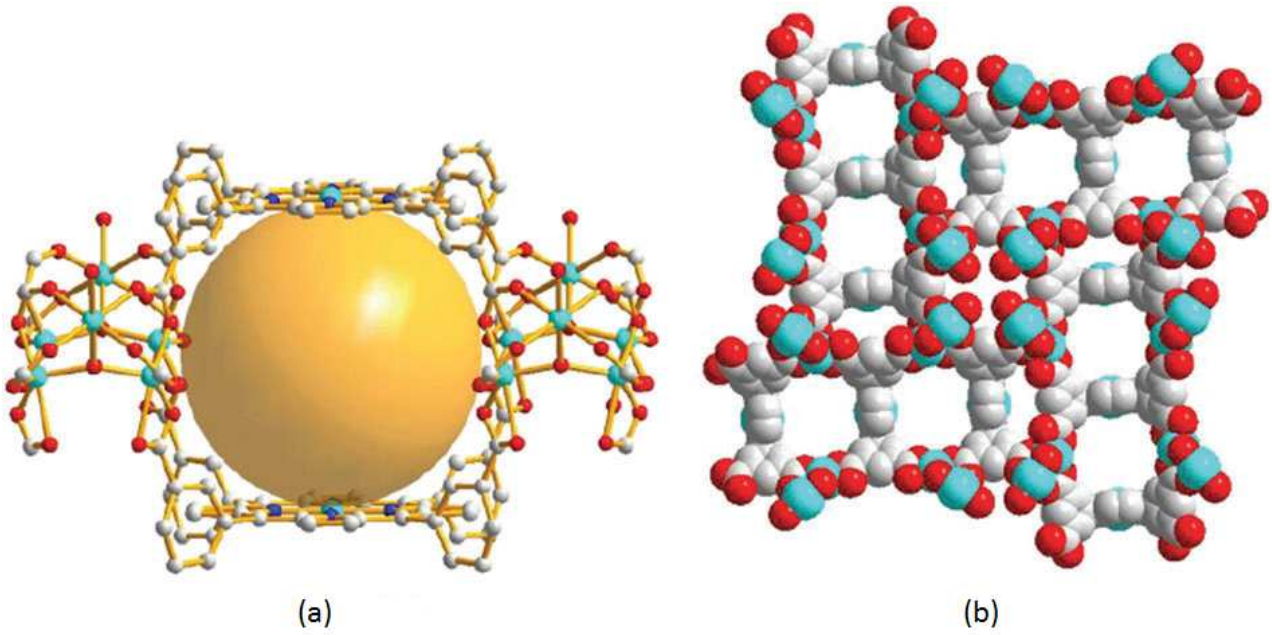

Fig. 3 (a) Three cobalt porphyrins located in the ‘‘face-to-face’’ configuration in MMPF-2; (b) space filling model of three types of channels in MMPF-2 viewed from the c direction.[54]

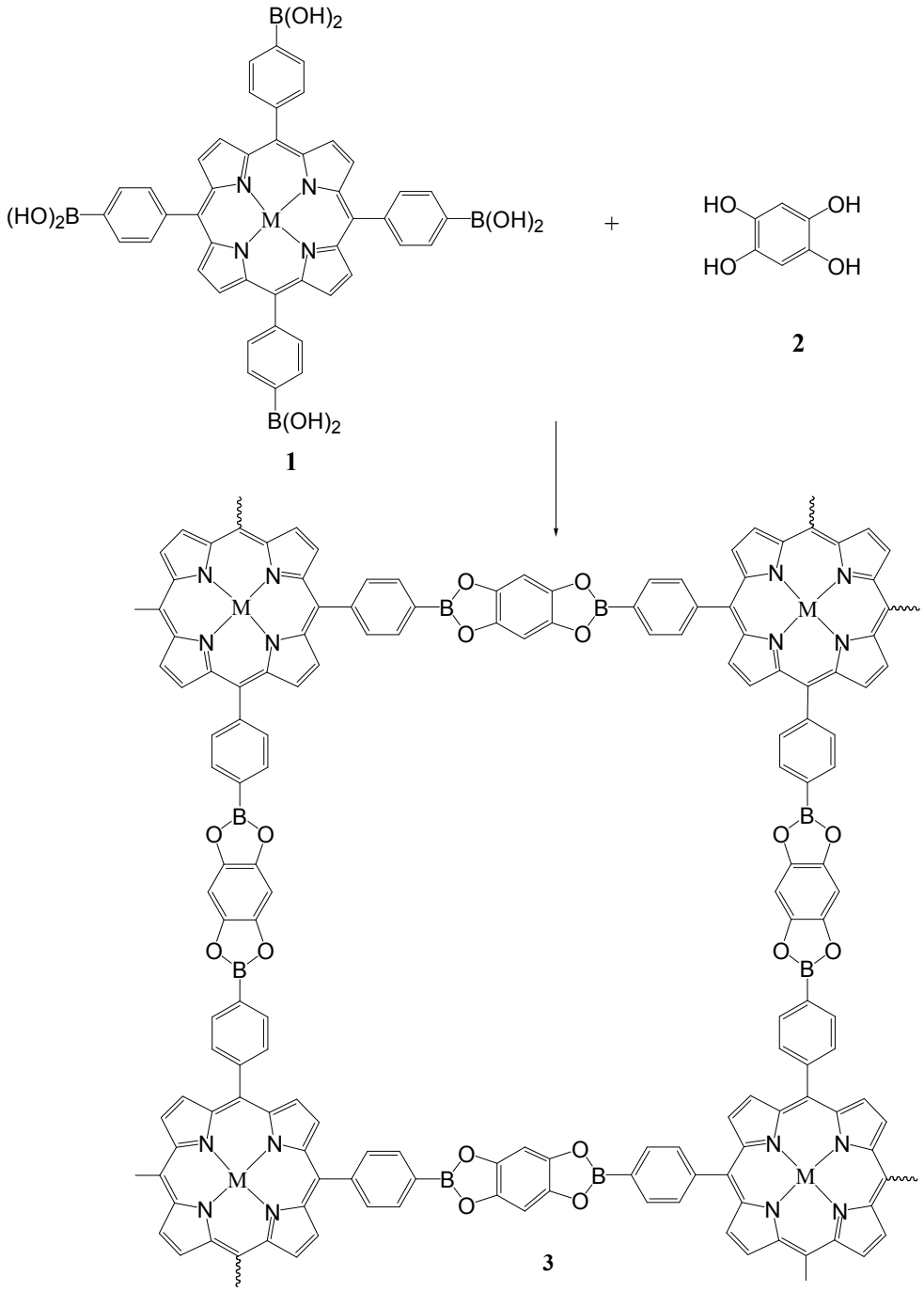

Fig. 4 Formation of porphyrin-based covalent-organic frameworks (COFs) (**6**).[67]

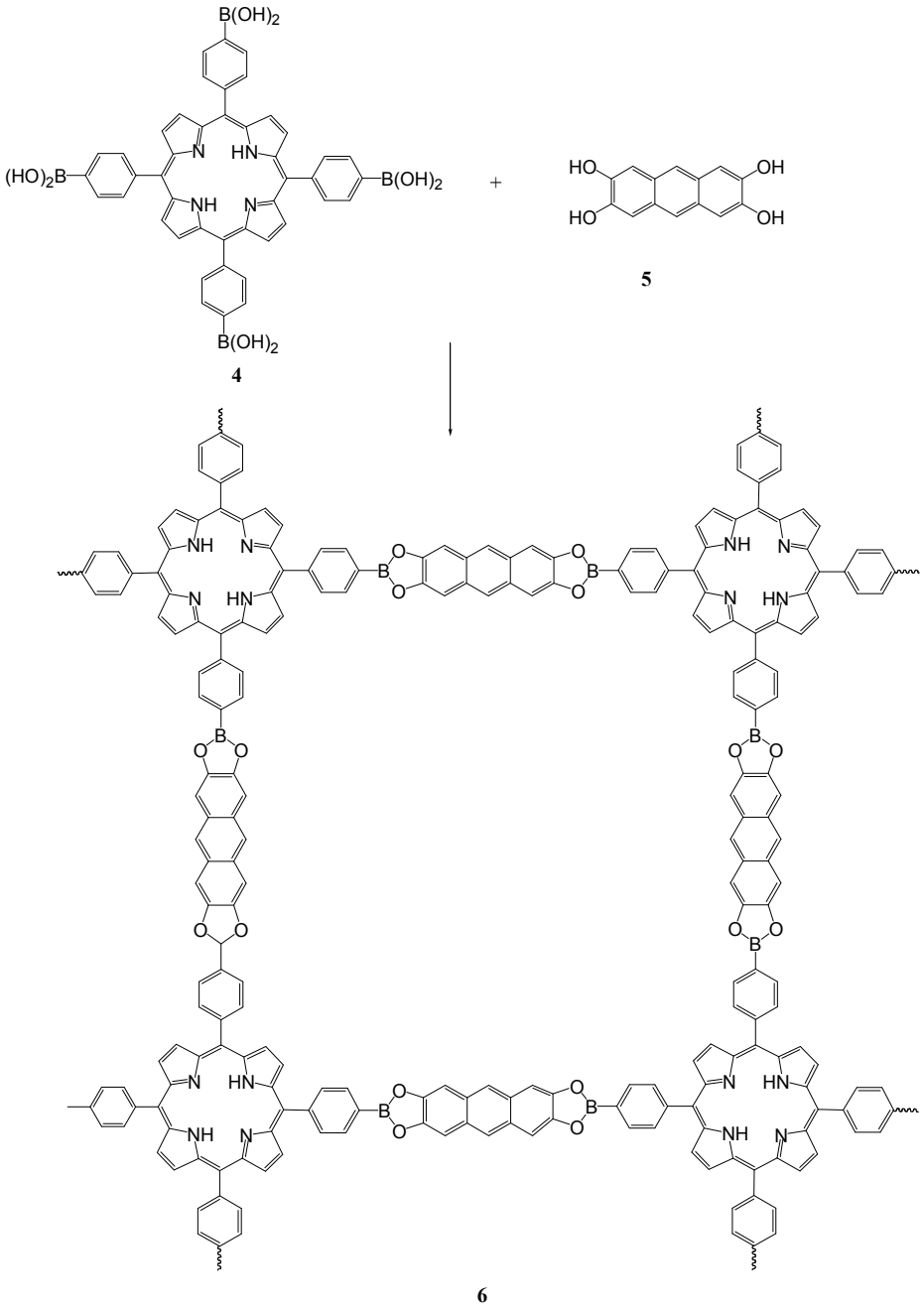

Fig. 5 Formation of porphyrin-based covalent-organic framework (COF-66) (**9**).[68]

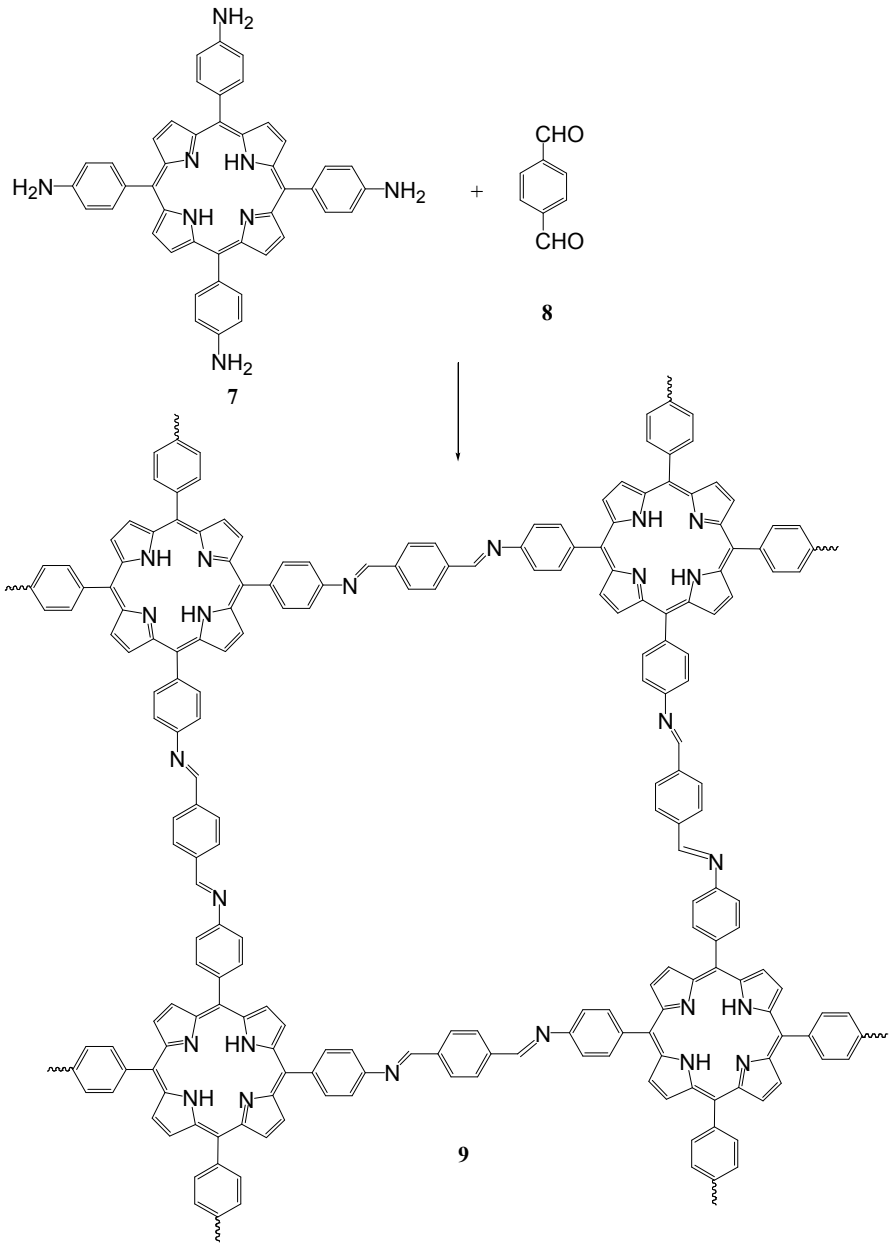

Fig. 6 Formation of porphyrin-based covalent-organic framework (COF-366) (**11**).[68]

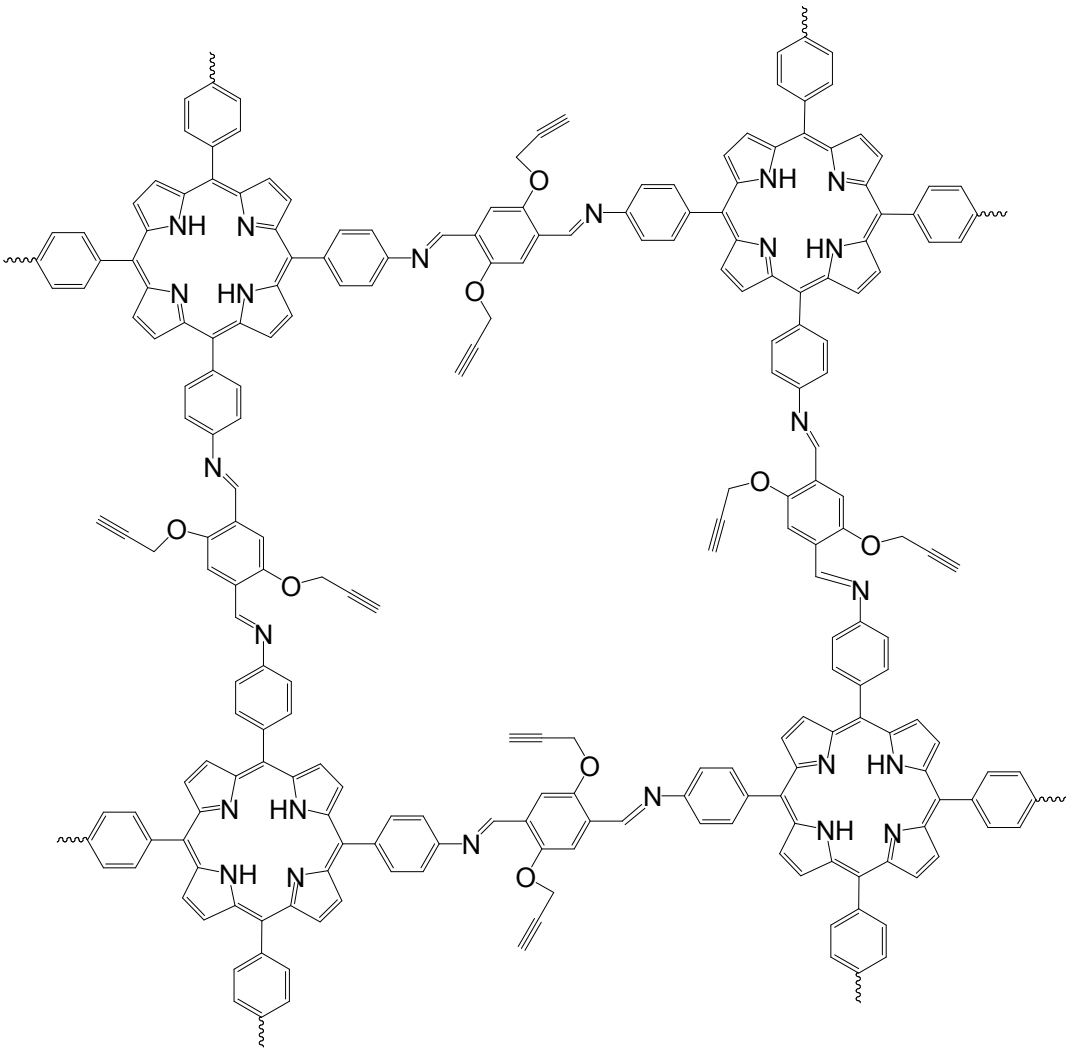

[CH≡C]x-H2P-COFs
(X= 0, 25, 50, 75, 100)

(a)

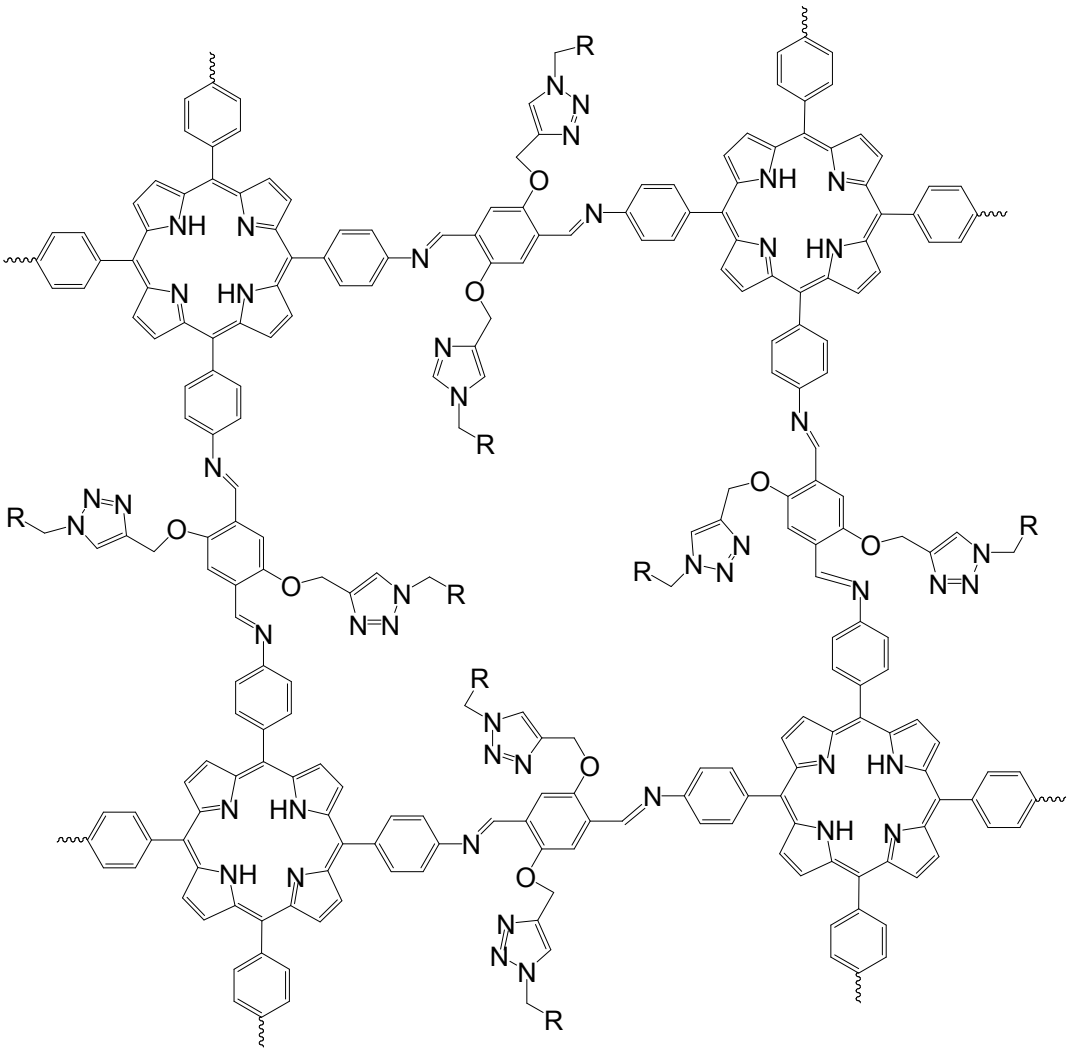

(b)

Fig. 7. Pore surface engineering of imine-linked COFs with various functional groups.[69]

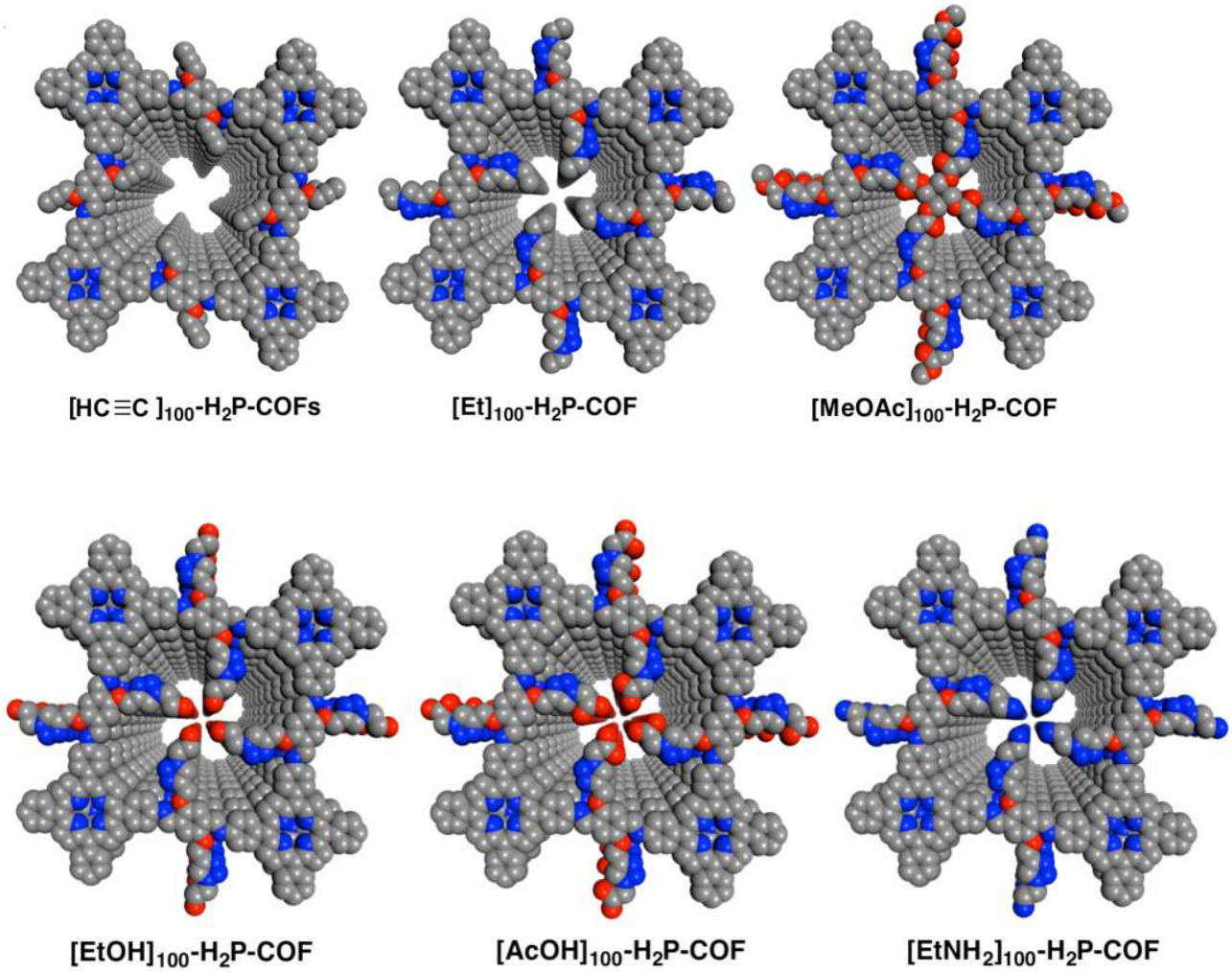

Fig. 8 Pore structures of COFs with different functional groups (Gray, C; Blue, N; Red, O) Adapted with permission from ([69]). Copyright (2015) American Chemical Society."

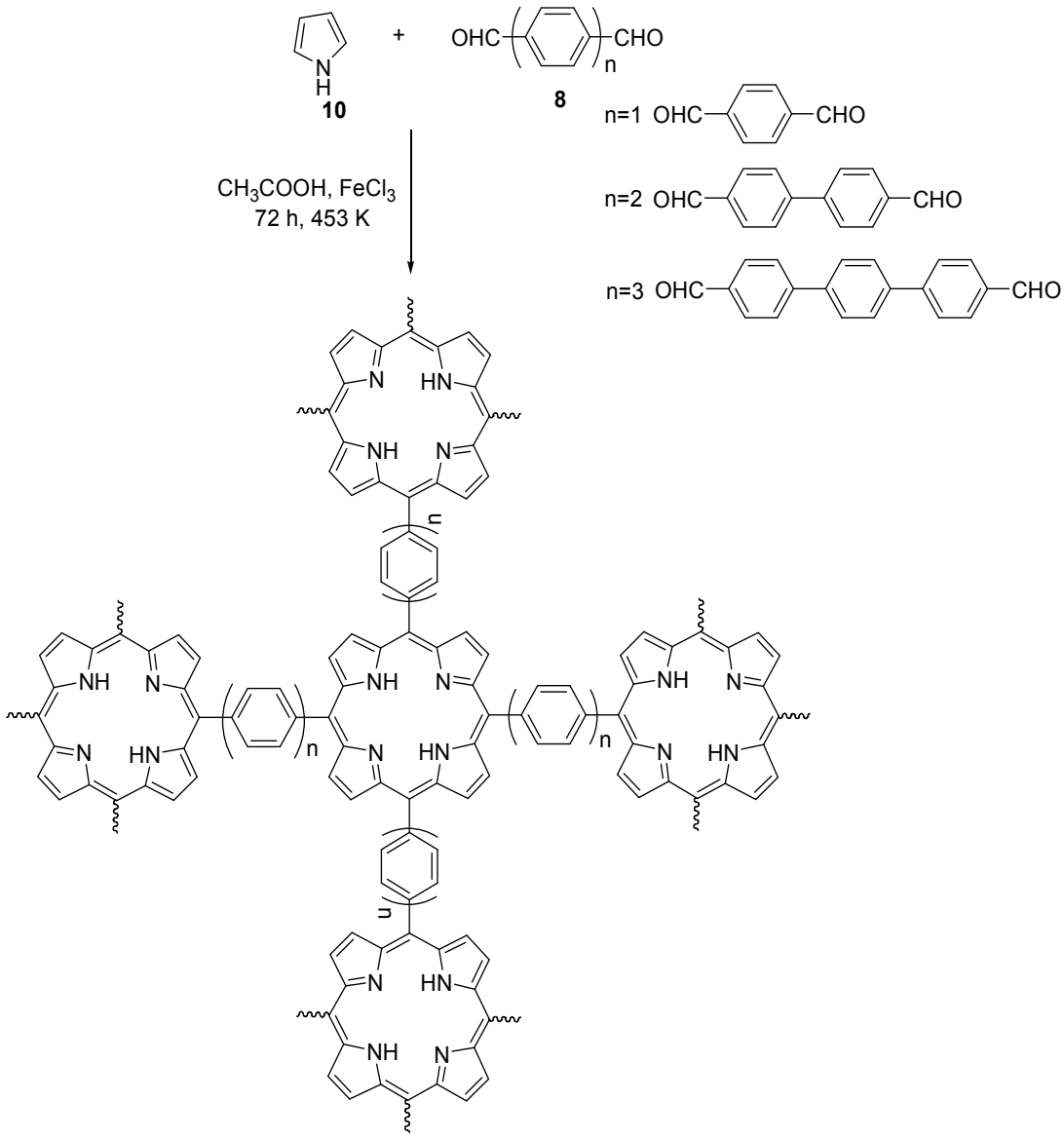

Fig. 9 Formation of molecular building blocks of iron containing porous organic polymers.[70]

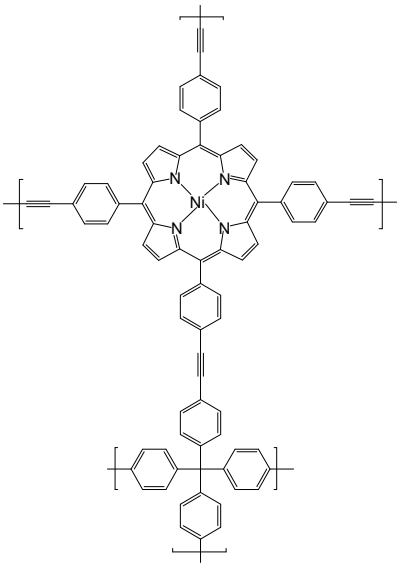

12

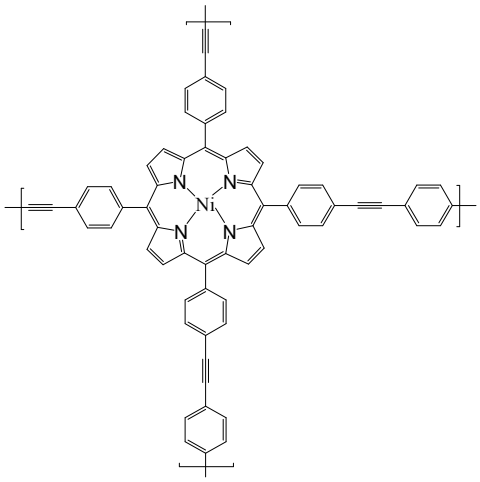

13

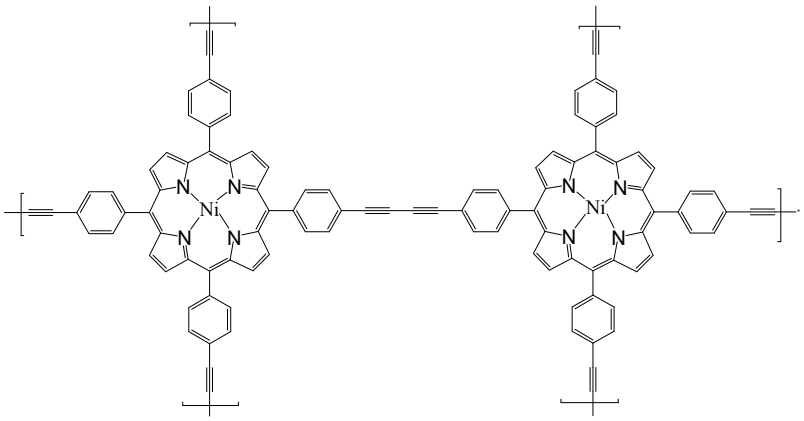

14

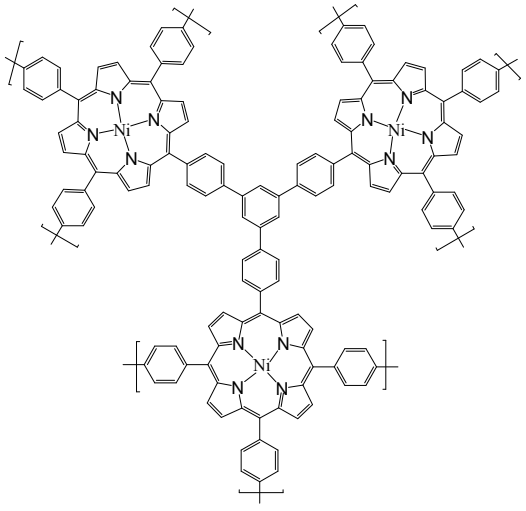

15

Fig.10 Structure of Ni-porphyrin dopped Polymers (**12, 13, 14, 15**).[72]

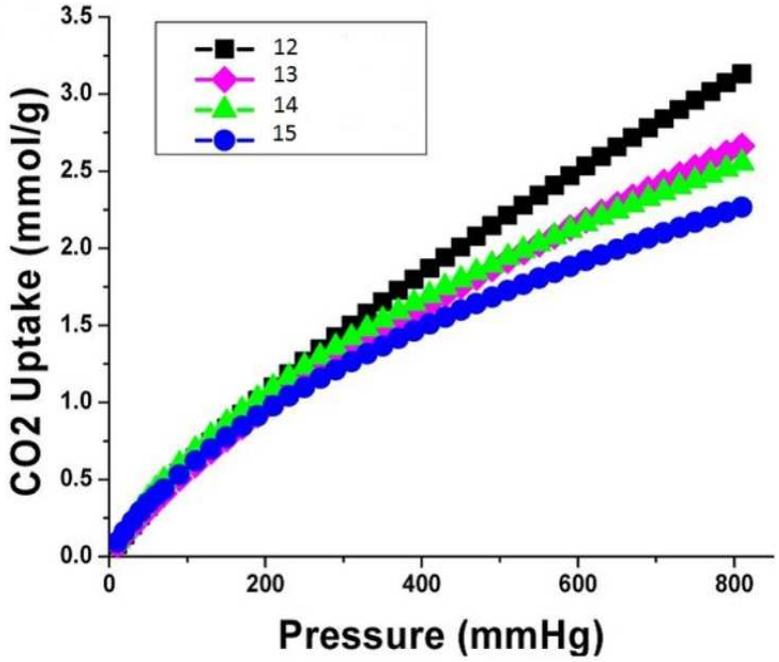

Fig.11 Carbon dioxide uptake isotherms of Ni-porphyrins at ice/water bath (with permission).[72]

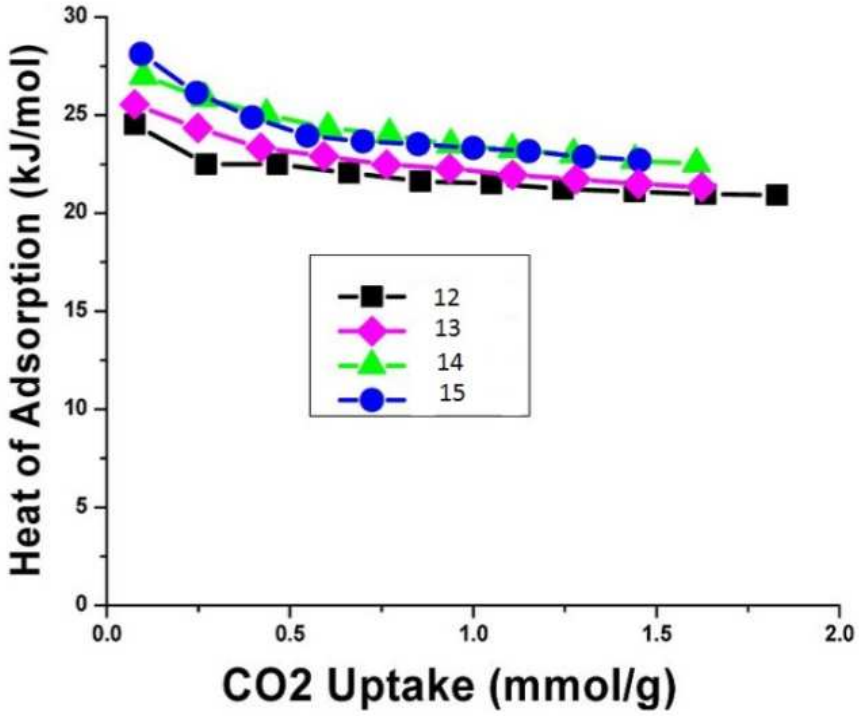

Fig.12 Heats of adsorptions of Ni-porphyrins as the function of carbon dioxide uptake (with permission).[72]

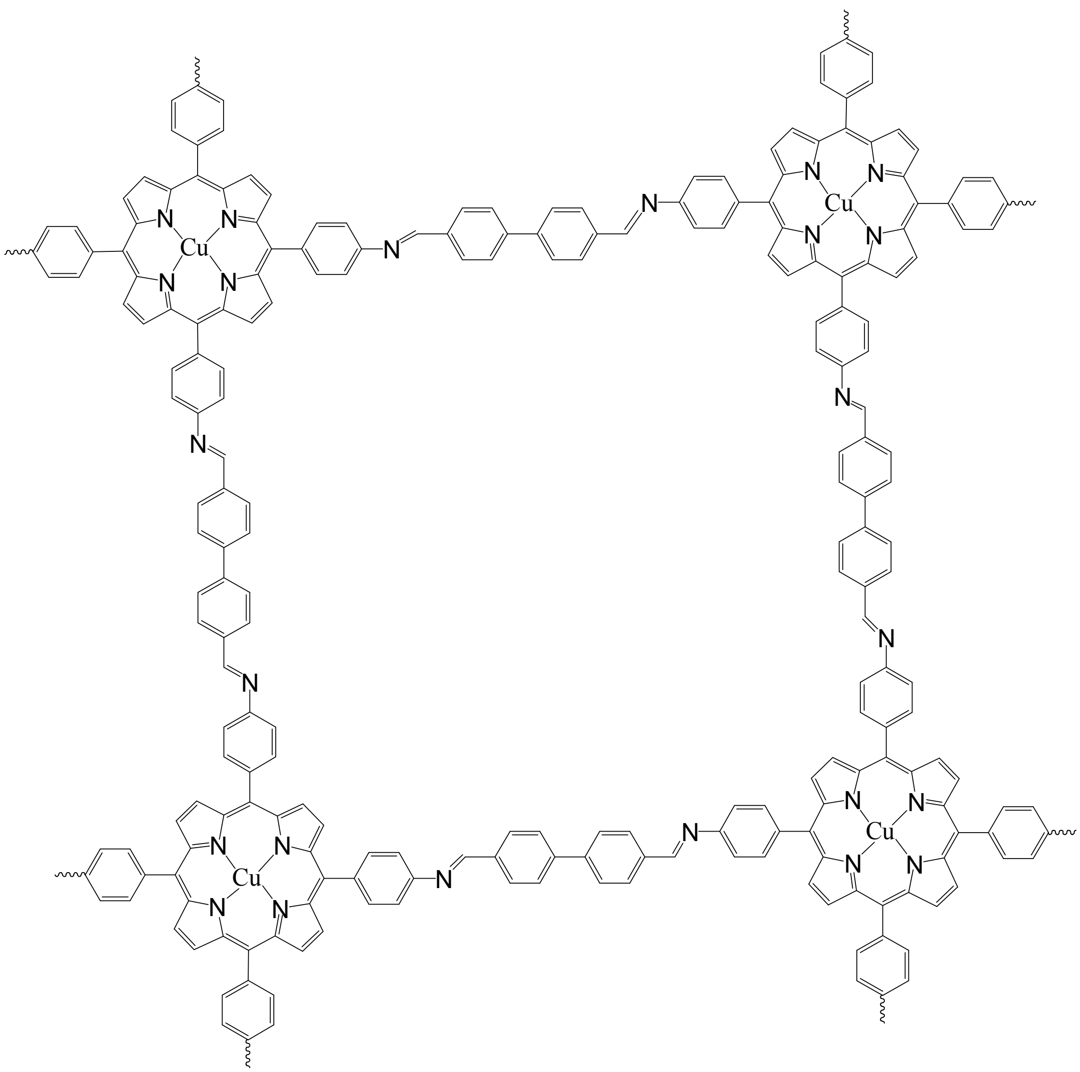

Fig. 13 Structure of CuPor-BPDC POP(**16**).[77]

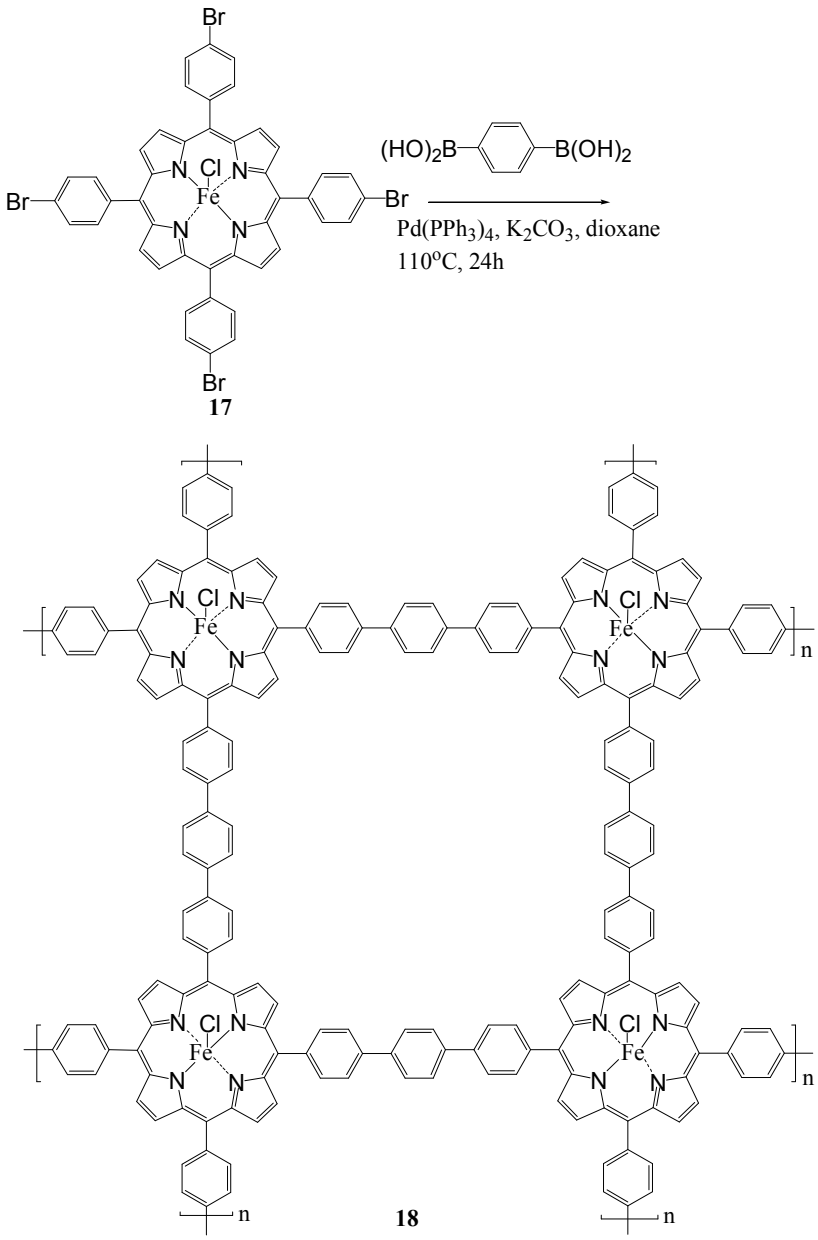

Fig. 14 The Synthesis of iron porphyrin conjugated microporous polymer (Fe-CMP-**18**).[79]

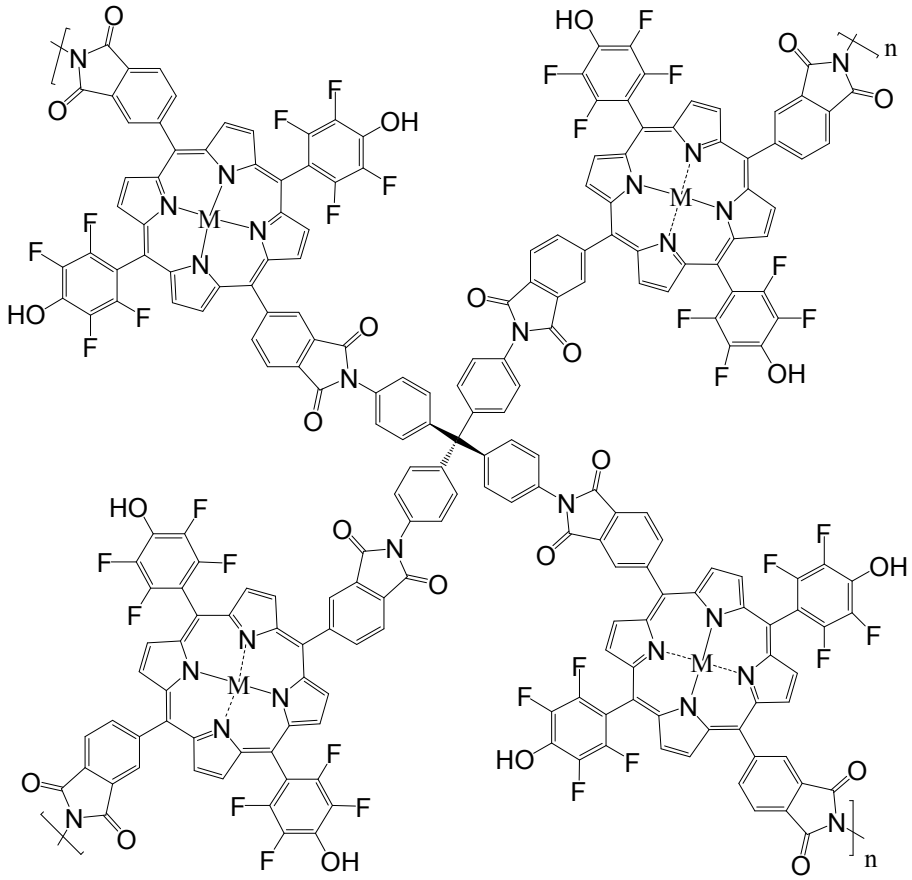

19

Fig. 15 Structure of metal porphyrin porous organic polymer (M = Fe and Mn).[80]

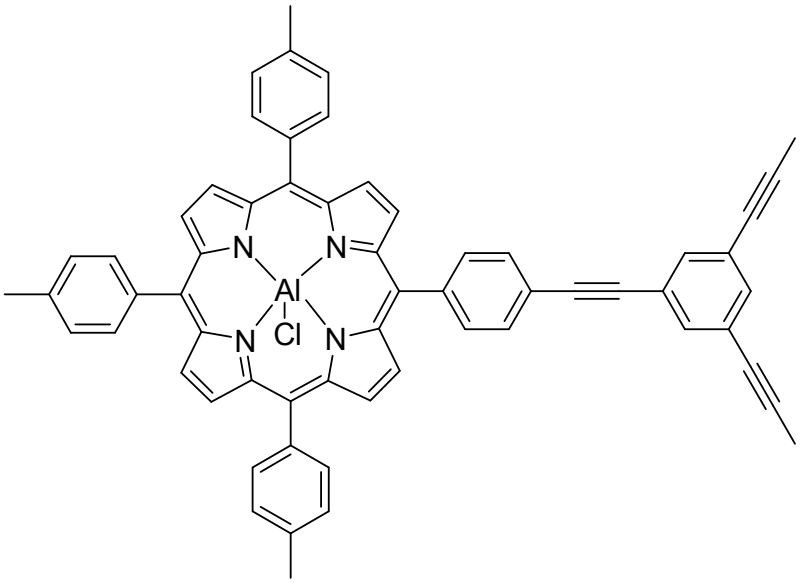

Fig. 16 Structure of metalloporphyrin-based conjugated microporous polymer (Al-CMP).

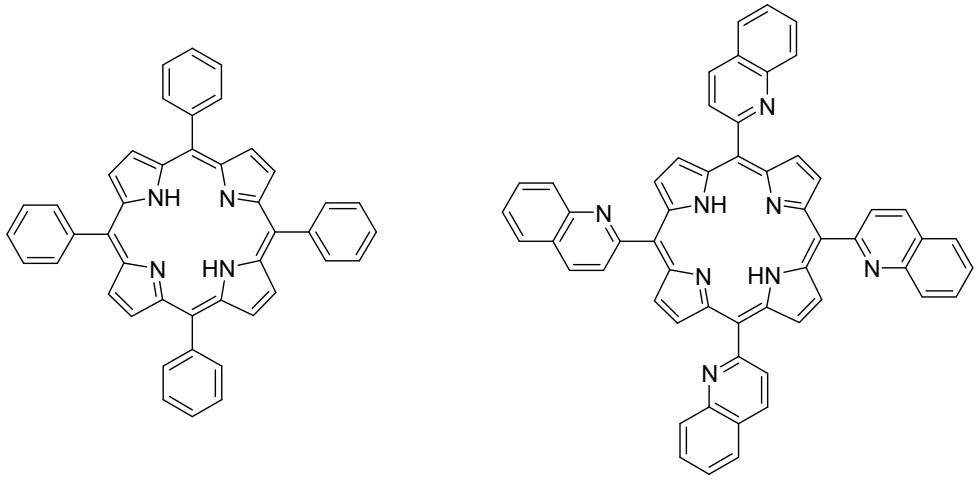

20 **21**

Fig. 17 Structure of meso-tetra-phenil-porphyrin-TPP (**20**) and meso-tetra-(2-quinolyl)-porphyrin-TQP (**21**).

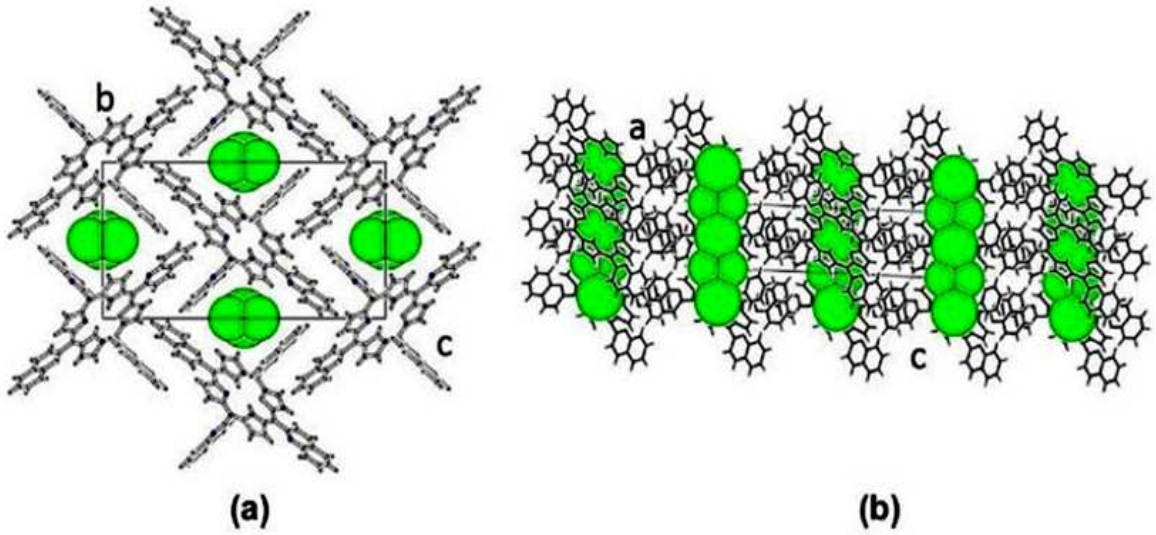

Fig.18 Packing diagram of TQP projected along a axis (left, a) and along the b axis (right, b). The larger green spheres represent the solvent accessible voids (with permission).[11]

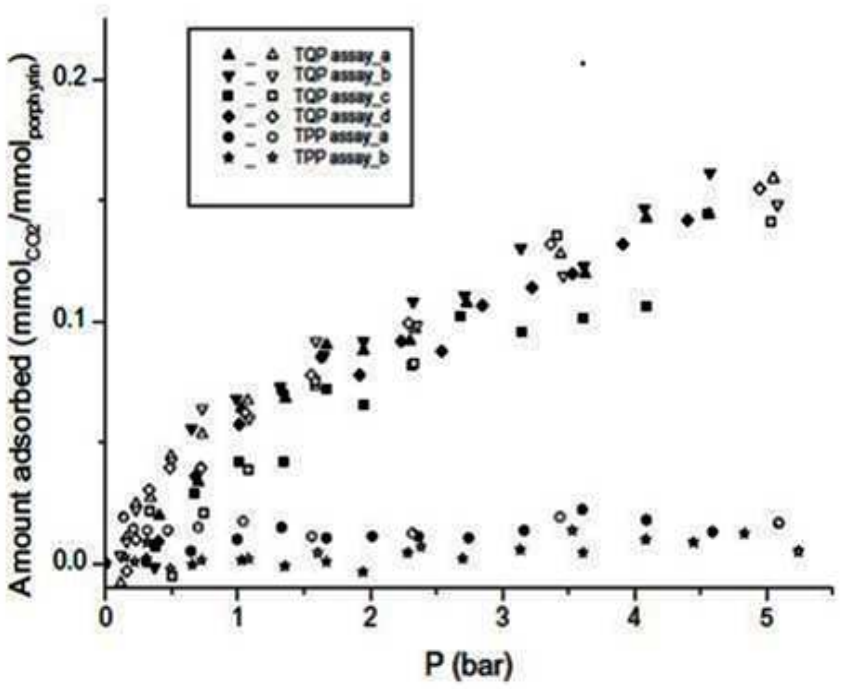

Fig.19 CO_2 adsorption (closed symbols)/desorption (open symbols) isotherms at 20 ^{o}C in crystalline TQP and TPP (with permission).[11]

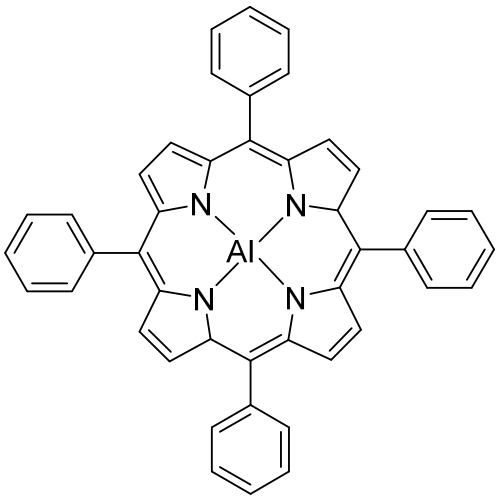

Fig.20 Porphyrin based homogeneous single-site catalyst for epoxide/CO_2 copolymerization.

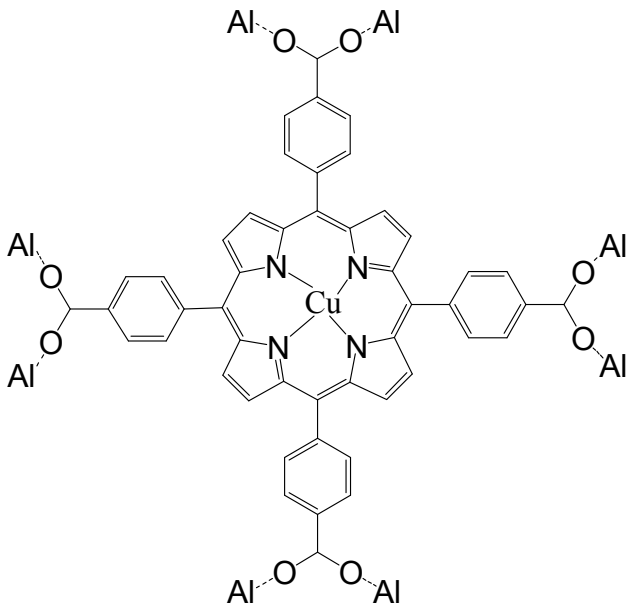

22

Fig.21 Structure of Cu porphyrin 5,10,15,20-Tetrakis(4-carboxyphenyl) porphyrin (Cu-TCPP).[112]

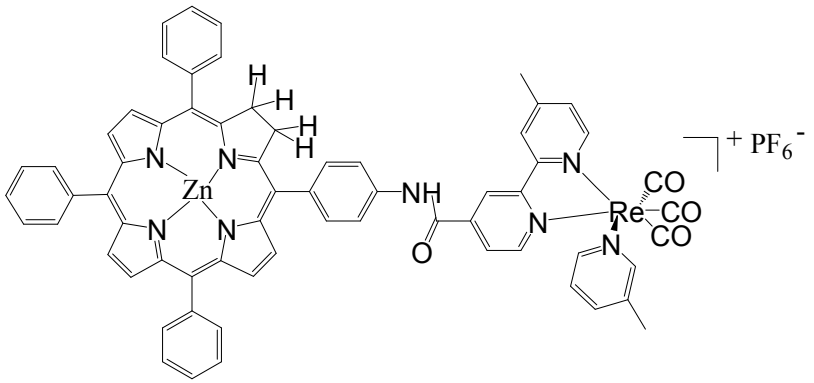

23

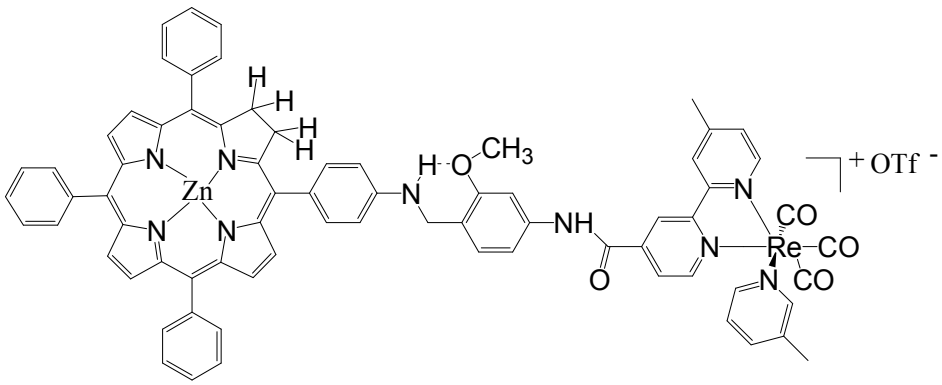

24

Fig. 22 Structure of dyad 1 (**23)** and dyad 2 (**24)** (with permission**).**[114]

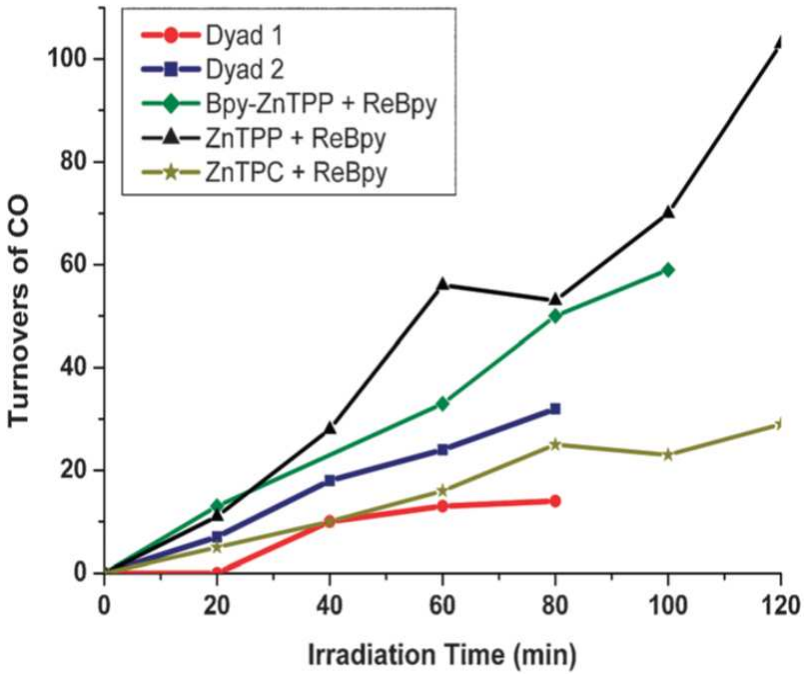

Fig. 23 Turnovers of CO generated on irradiation of photocatalysts under 1 atm CO_2 in DMF/TEOA (5 : 1) 0.05 mM catalyst, ReBpy = $[Re(CO)_3(Pic)Bpy][PF_6]$ (with permission). [114]

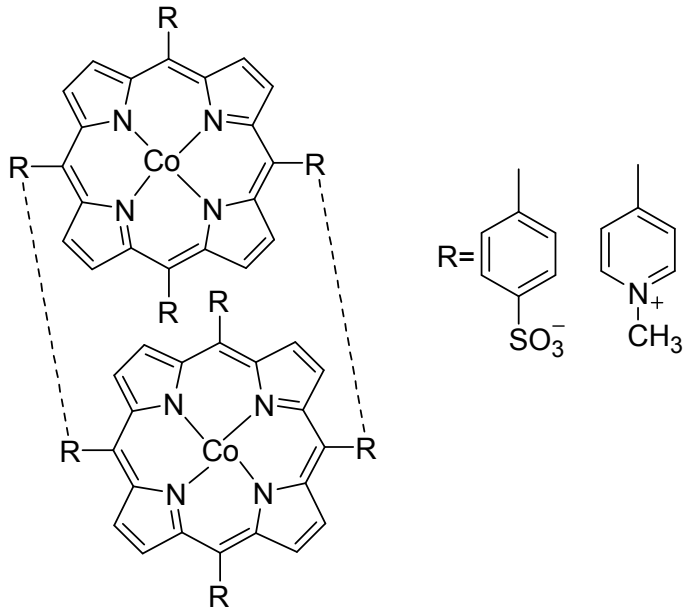

Fig. 24 Self-assembled Co co-facial bis-porphyrins.

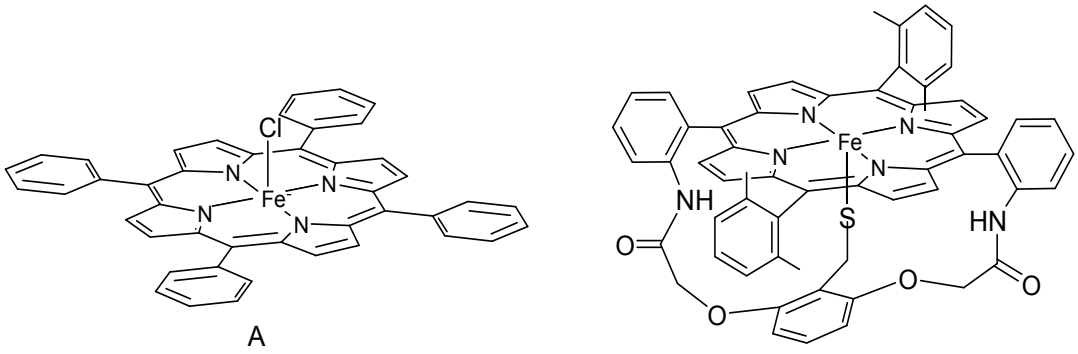

Fig. 25 Structure of meso-tetra phenyl porphyrin Fe (III) chloride (**A**) or the thiolate basket porphyrin (**B**) complexes.[118]

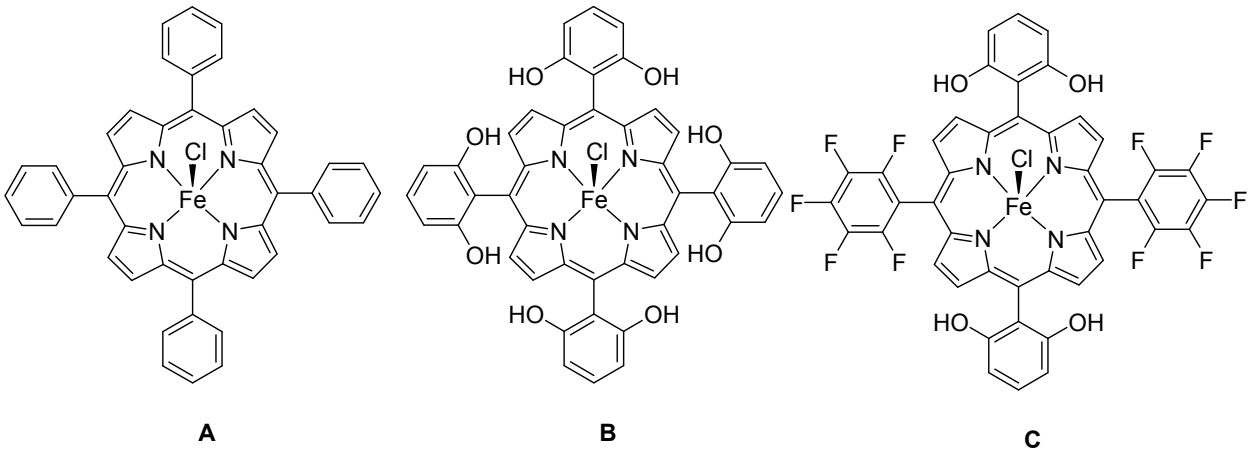

Fig. 26 Iron porphyrin catalysts (A) Iron(III) 5,10,15,20-tetraphenylporphyrin chloride; (B) chloro iron(III) 5,10,15,20-tetrakis(2',6'-dihydroxyphenyl) porphyrin chloride and (C) pentafluorinated [chloro iron(III) 5,15-bis(2',6'-dihydroxyphenyl)-10,20-bis(pentafluorophenyl) porphyrin.

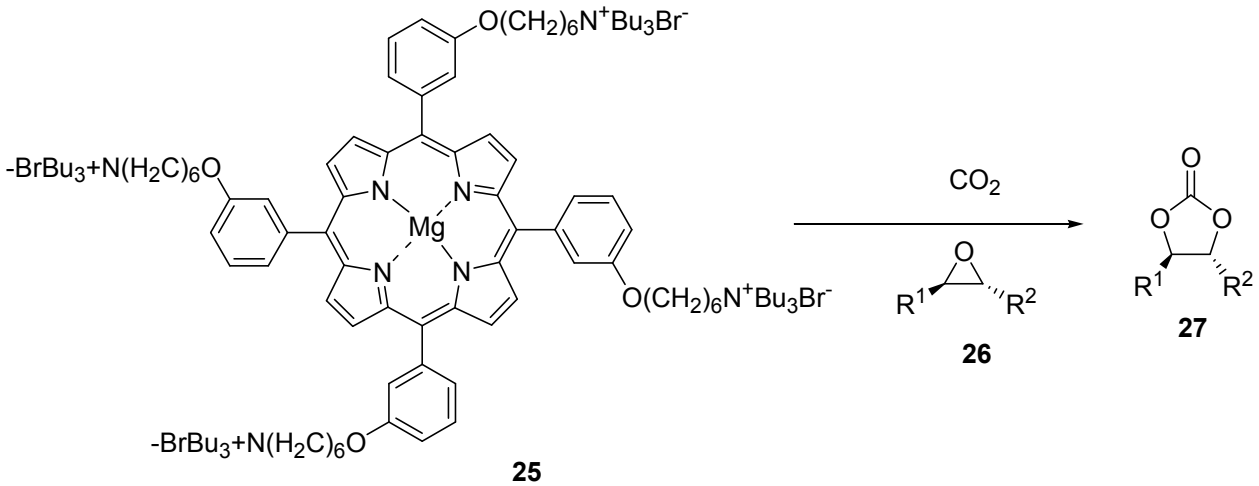

Fig. 27 Synthesis of cyclic carbonate **27** from epoxide **26** and CO_2.[127]

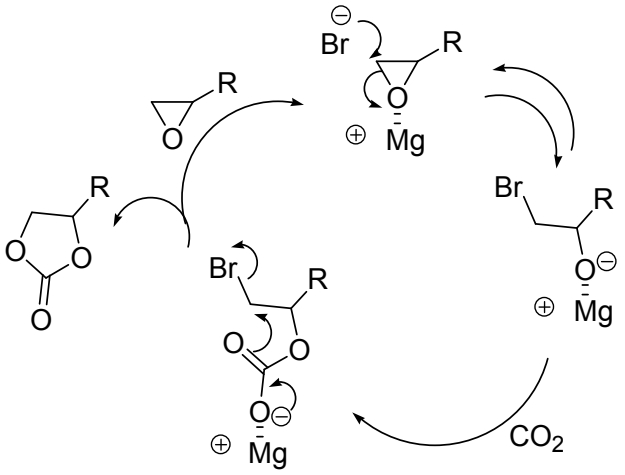

Fig. 28 A plausible catalytic cycle (with permission).[127]

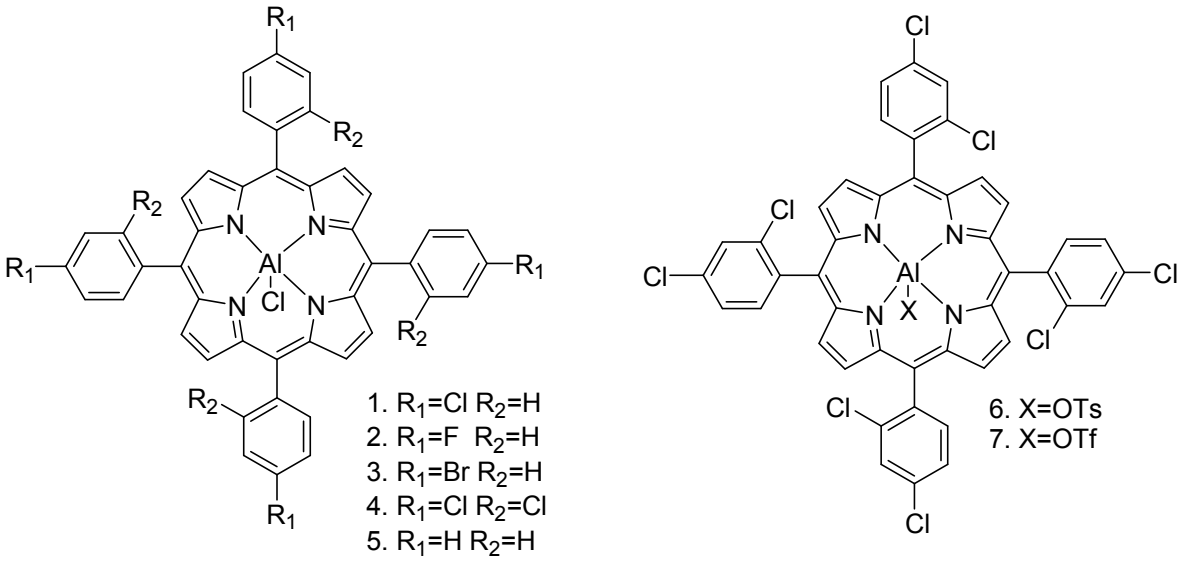

Fig.29 Aluminum porphyrin complexes.[130]

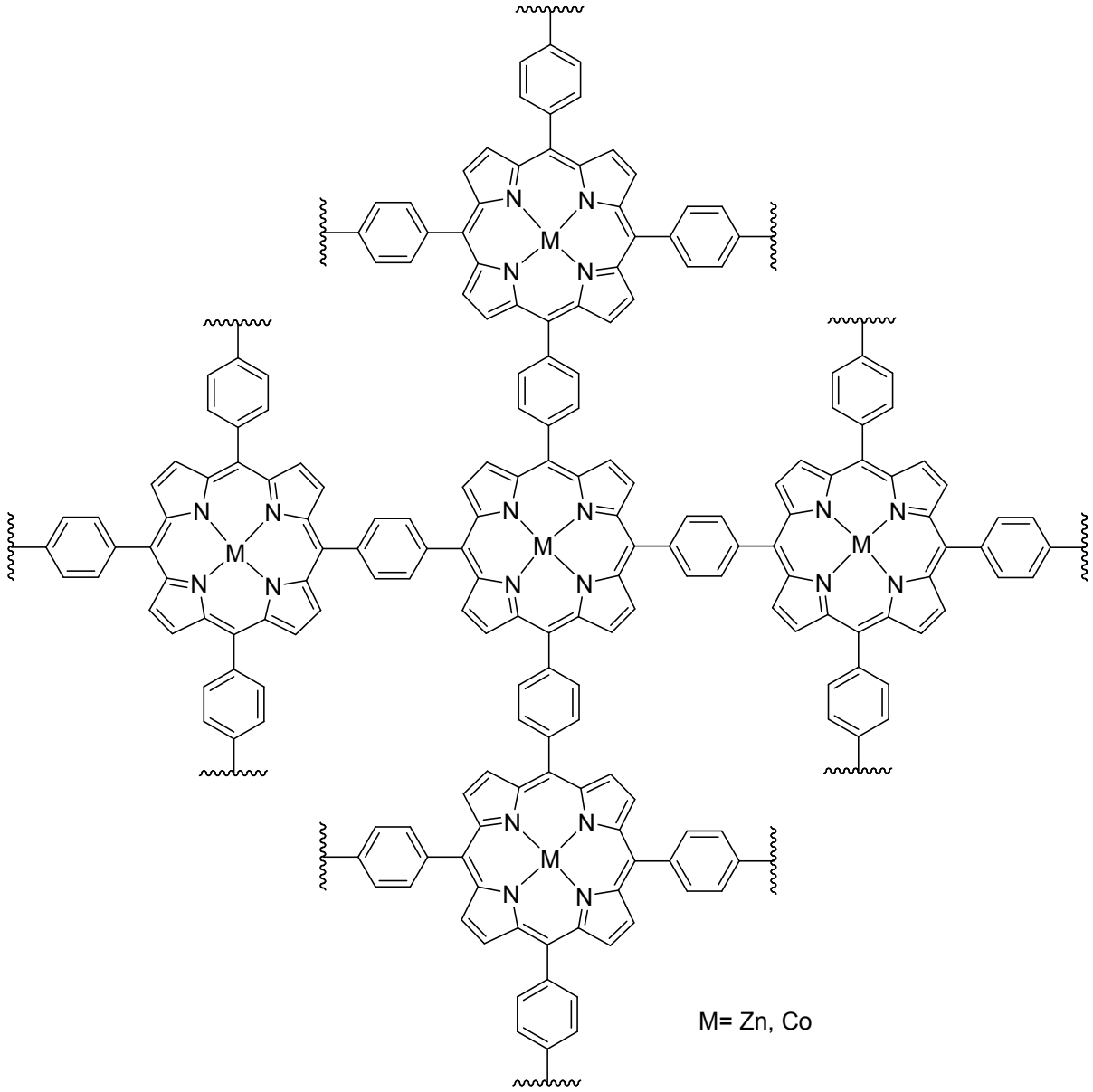

Fig. 30 Structure of metalloporphyrin catalyst.[131]

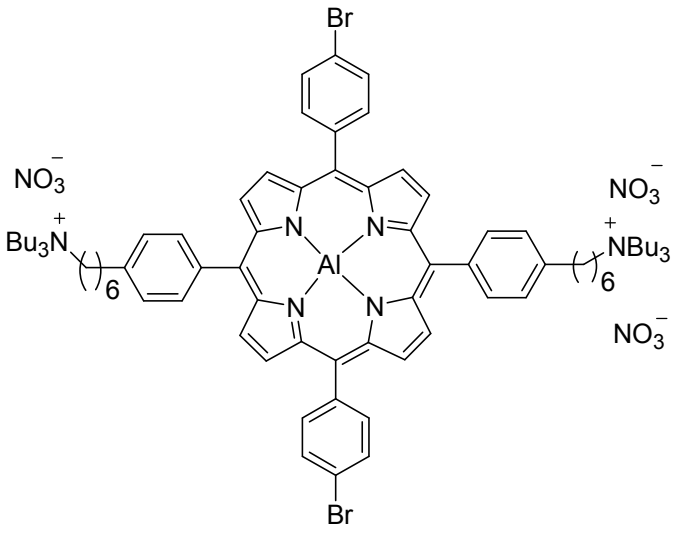

Fig.31 Structure of the bifunctional aluminum porphyrin complex.

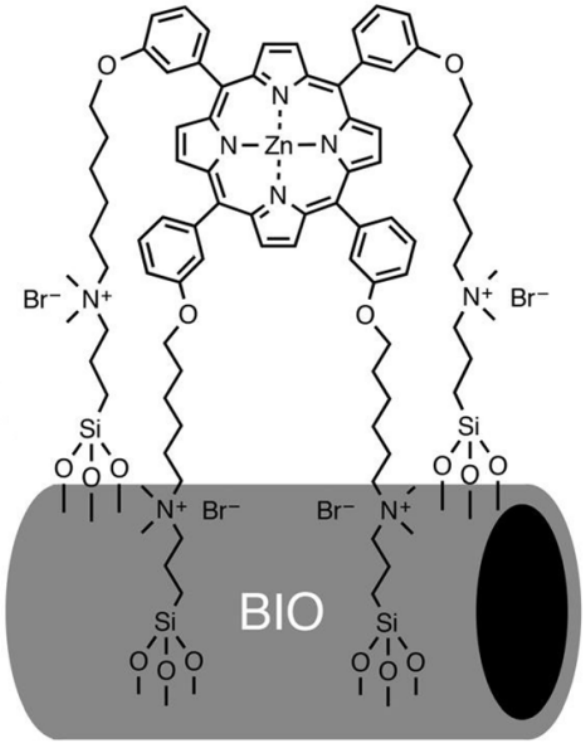

Fig. 32 Zn(II) porphyrin linked to BIO via four tetra-alkyl ammonium bromide groups (with permission).[138]

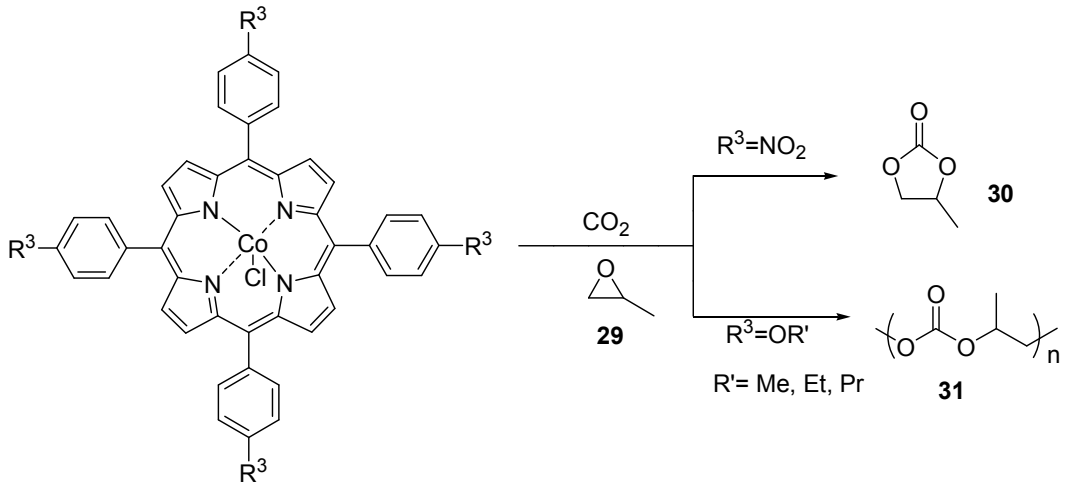

Fig. 33 Synthesis of cyclic carbonate **30** and poly propylene carbonate **31** from epoxide **29** and CO_2.

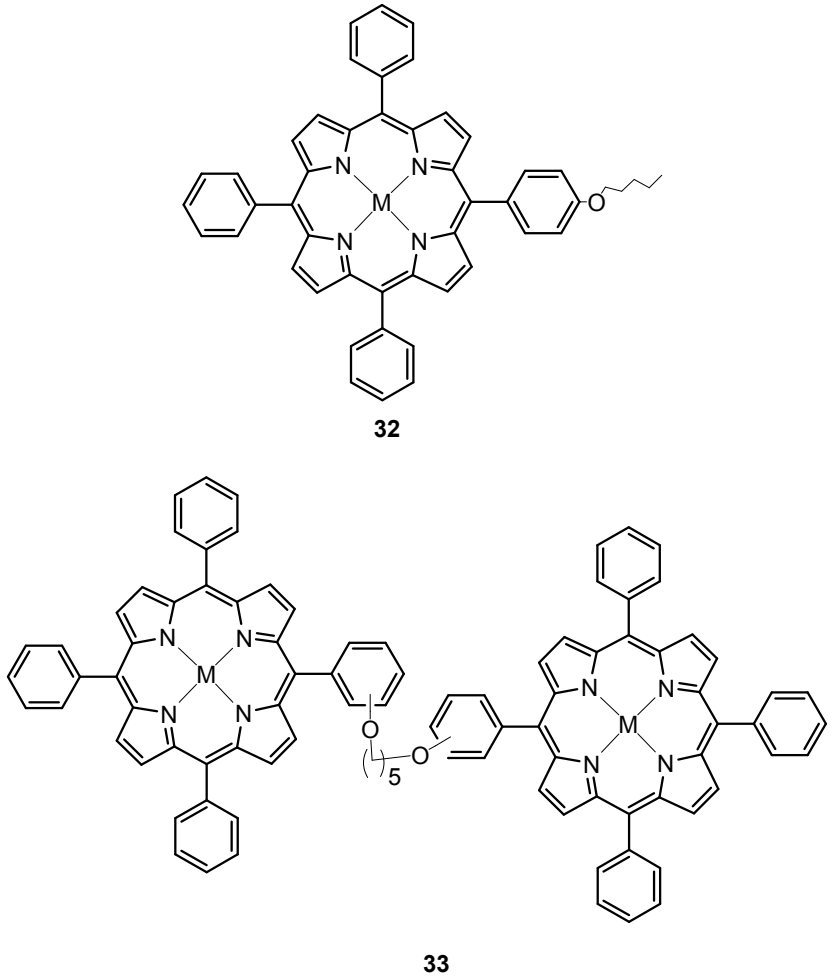

Fig. 34 Structure of mononuclear cobalt porphyrin (**32**) and bis-para-tethered cobalt bis-porphyrin (**33**).[141]

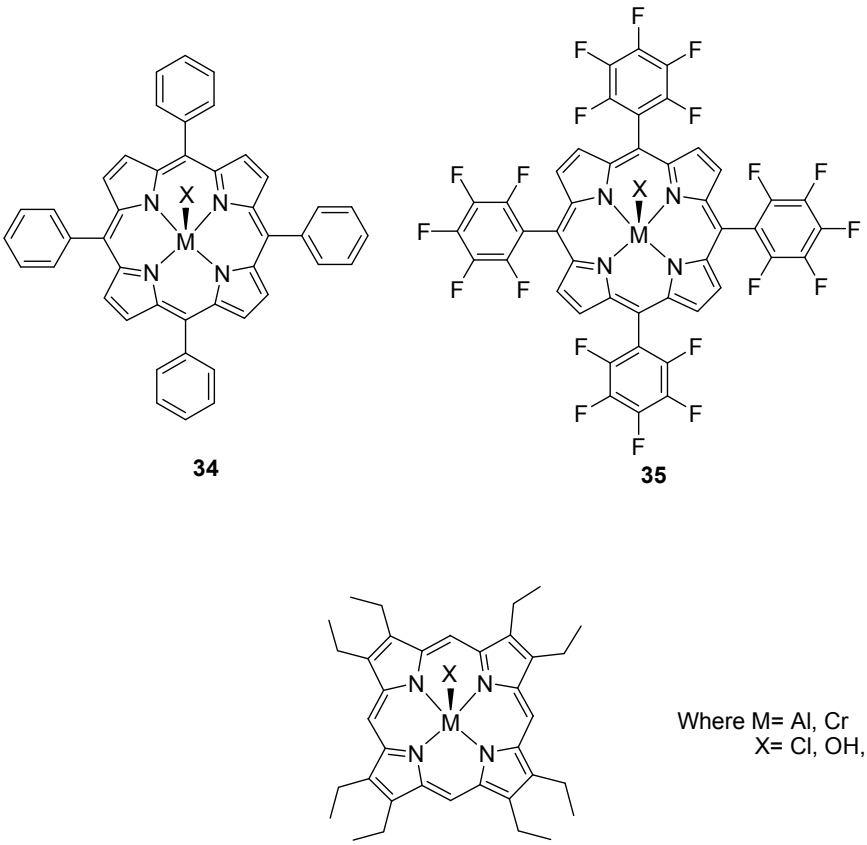

Fig. 35 Structure of porphyrin catalyst (**34**) 5,10,15,20-tetraphenylporphyrin; (**35**) 5,10,15,20-tetrakis(pentafluorophenyl)porphyrin; and (**36**) 2,3,7,8,12,13,17,18-octaethylporphyirn for conversion of CO_2 to propylene carbonate and polypropylene carbonate.

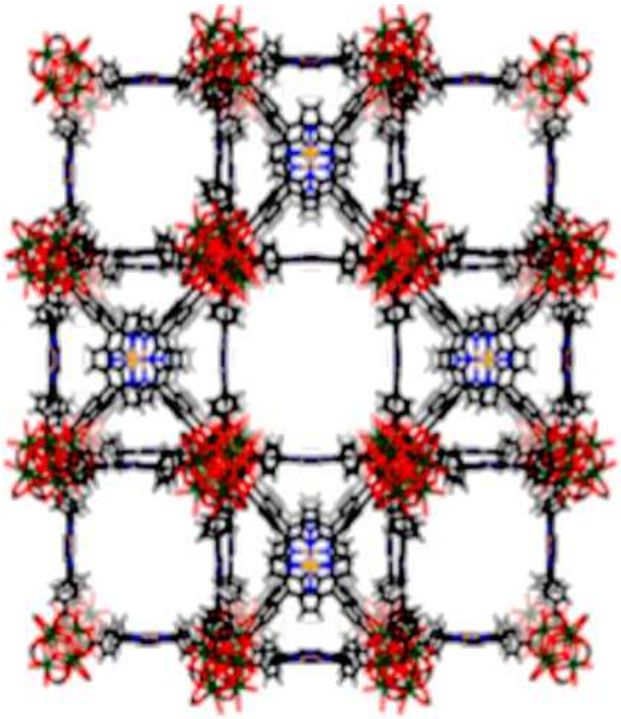

Fig. 36 Strucure of cobalt porphyrin zirconium MOF, PCN-224 (Co) 3D nanochannels (with permission). [147]

Table 1. Summary of porphyrin based porous materials in term of surface area, porosity and the capacity of CO_2 uptake

Entry	Materials	BET surface area (m^2g^{-1})	Pore volume (Vp cm^3g^{-1})	CO_2 uptake at 273K	References
1	$[HC\equiv C]_0$-H2PCOF	1474	0.75	72 mgg^{-1}	69
2	$[HC\equiv C]_{25}$-H2PCOF	1413	0.71	54 mgg^{-1}	69
3	$[HC\equiv C]_{50}$-H2PCOF	962	0.57	48 mgg^{-1}	69
4	$[HC\equiv C]_{75}$-H2PCOF	683	0.42	43 mgg^{-1}	69
5	$[HC\equiv C]_{100}$-H2PCOF	462	0.28	39 mgg^{-1}	69
6	$[Et]_{25}$-H2PCOF	1326	0.55	55 mgg^{-1}	69
7	$[Et]_{50}$-H2PCOF	821	0.48	46 mgg^{-1}	69
8	$[Et]_{75}$-H2PCOF	485	0.34	41 mgg^{-1}	69
9	$[Et]_{100}$-H2PCOF	187	0.18	38 mgg^{-1}	69
10	$[MeOAc]_{25}$H2PCOF	1238	0.51	84 mgg^{-1}	69
11	$[MeOAc]_{50}$H2PCOF	754	0.42	88 mgg^{-1}	69
12	$[MeOAc]_{75}$H2PCOF	472	0.31	82 mgg^{-1}	69
13	$[MeOAc]_{100}$H2PCOF	156	0.14	65 mgg^{-1}	69
14	$[AcOH]_{25}$-H2PCOF	1252	0.52	94 mgg^{-1}	69
15	$[AcOH]_{50}$-H2PCOF	866	0.45	117 mgg^{-1}	69
16	$[AcOH]_{75}$-H2PCOF	402	0.32	109 mgg^{-1}	69
17	$[AcOH]_{100}$-H2PCOF	186	0.18	96 mgg^{-1}	69
18	$[EtOH]_{25}$-H2PCOF	1248	0.56	92 mgg^{-1}	69
19	$[EtOH]_{50}$-H2PCOF	784	0.43	124 mgg^{-1}	69
20	$[EtOH]_{75}$-H2PCOF	486	0.36	117 mgg^{-1}	69
21	$[EtOH]_{100}$-H2PCOF	214	0.19	84 mgg^{-1}	69
22	$[EtNH_2]_{25}$-H2PCOF	1402	0.58	116 mgg^{-1}	69
23	$[Et\ NH_2]_{50}$-H2PCOF	1044	0.50	133 mgg^{-1}	69
24	$[Et\ NH_2]_{75}$-H2PCOF	568	0.36	157 mgg^{-1}	69
25	$[EtNH_2]_{100}$-H2PCOF	382	0.21	97 mgg^{-1}	69

26	POP-1	875	1.1	19.0 wt%	70
27	POP-2	855	1.04	18.6 wt%	70
28	POP-3	750	0.75	9.0 wt%	70
29	POP-4	560	0.44	27.3 wt%	71
30	Ni-Por-1 POP (14)	1711	0.90	3.13 $mmolg^{-1}$	72
31	Ni-Por-2POP (15)	1393	0.96	2.66 $mmolg^{-1}$	72
32	Ni-Por-3POP (16)	894	0.59	2.55 $mmolg^{-1}$	72
33	Ni-Por-4POP (17)	778	0.62	2.26 $mmolg^{-1}$	72
34	CMPF	662	0.55	3.58 $mmolg^{-1}$	74
35	CuPor-BPDC (18)	442	0.41	5.5 wt%	77
36	FeP-CMP (21)	1270	1.18		79
37	MMPF-2	1410	0.61	33.4 wt%	54
38	MMPF-4	958		24.4 wt%	55
39	MMPF-7	600		10.7 wt%	81
40	MMPF-8	910		16.2 wt%	81
41	Al-CMP	839	839	4.3 wt%	82

Table 2. Synthesis of cyclic carbonate (**28**) from carbondioxide and epoxide (**27**) with Mg(II) porphyrin catalyst (**26**).[127]

Entry	27	R^1	R^2	Time/h	Yield[a] (%)
1	27a	Bu	H	3	99
2	27b	Me	H	6	99
3	27c	Oct	H	6	93
4	27d	Ph	H	9	93
5	27e	CH_2Cl	H	6	95
6	27f	CH_2OMe	H	9	95
7	27g	CH_2OPh	H	9	98
8	27h	CH_2OH	H	9	87
9	27i	$CH{=}CH_2$	H	9	81
10	27j	Bu	D	6	72

[a]Isolated yield

Graphical Abstract